LUNDS UNIVERSITET
Lunds Tekniska Högskola

Department of Atomic Physics
Quantum information group

Fiber noise cancellation

Thesis work
Master of engineering, Nanoscience.
LRAP-461

Author:
Anders Rönnholm

Supervisor:
Lars Rippe

Lund 120614

Abstract

In a quantum information system one single or group of ions can be used as a qubit. To manipulate the qubits a laser pulse is used. Because of the small dimensions the laser beam cannot be directed to physically hit just one single qubit. Instead the qubits are "programmed" to listen to each one's specific frequency.

The frequency of the laser pulse is tuned to address different qubits and the frequency stability of the laser pulse is of absolute importance. Even the small frequency shifts occurring from optical fibers (fiber noise), used to direct the beam, have significant impact of stability.
This report describes one technic to cancel the fiber noise. The theory is quite basic and is based on a negative feedback loop.

The laser beam is sent through the optical fiber where a partly transparent mirror reflects a small part of the beam back a second time through the fiber. The phase noise in the reflected beam is measured by a photo detector, and the error signal is sent to a regulator controlling an optic frequency modulator.
The laser beam is thus pre-regulated with the same phase noise, but inverted, that induced in the fiber cable, before it enters the same fiber cable, causing the outgoing laser beam to be theoretically fiber noise free.
This requires that the system regulation speed is substantially faster than the changes in the fiber noise.
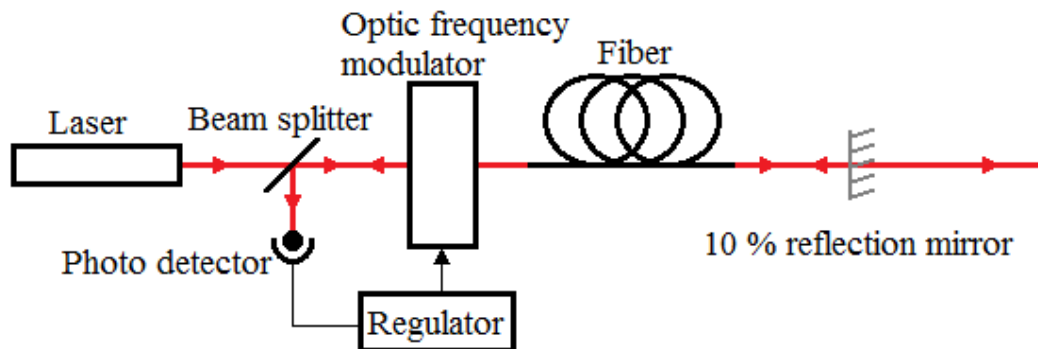
Figure 1. *Fiber noise cancellation schematic.*

The thesis work has progressed over a period of five month and has included planning and calculations, purchases, building of system and measuring of noise suppression.

Populärvetenskaplig sammanfattning.

I kvantvälden får vi vänja oss vid att det som verkar omöjligt kan vara möjligt. Till exempel kan en partikel vara på fler än ett ställe samtidigt vilket i den synliga världen verkar vara rent trams. Men faktum är att kvantmekanikens "trams" har visat sig stämma överens med experiment efter experiment. Just att en atom, eller grupp av atomer, kan befinna sig på flera ställen samtidigt, eller kan ha flera olika tillstånd samtidigt, utnyttjas vid kvantdatorforskning. En traditionell dator arbetar med bitar som har värde 1 eller 0, men en bit i en kvantdator, kvantbit, kan vara 1 och 0 samtidigt och på så vis göra flera beräkningar parallellt.

På grund av storleken är det svårt att sätta och läsa av kvantbitarna med hjälp av elektriska kontakter. Istället används en laser. Laserstrålen är också för bred för att rikta in sig på en enskild kvantbit, men varje kvantbit är inställd att lyssna till en viss frekvens. Problemer är att frekvenserna ligger så pass tätt att lasern måste vara extremt brusfri och stabil för att inte träffa fler än en kvantbit åt gången. Laserfrekvensen ligger på hundratals Terahertz (för synligt ljus) och brus på några kHz, i vissa system ner till några tiotals Hz är tillräckligt för att störa experimenten.

En optisk fiber används ofta för att leda en laserstråle eftersom den är flexibel och har låg inverkan på lasern. På grund av vibrationer, tryck- och temperaturväxlingar ändras geometrin i den optiska fibern vilket i sin tur påverkar laserstrålen genom fibern. Dessa störningar är i de flesta fall helt försumbara, men i en extremt stabiliserad laser är störningarna ett problem och måste kompenseras bort.

Detta exjobb har gått ut på att konstruera och tillverka ett system för att kompensera bort fiberbrus. Principen är ganska enkel och kan beskrivas som ett negativt återkopplingssystem. Felet(fiberbruset) mäts och skickas till en optisk frekvensmodulator som justerar signalen(laserfrekvensen) med samma värde som felet, men inverterat. Den brusfria laserstrålen får alltså en störning adderad innan den går in i fiberkabeln där bruset tar ut störningen vilket ger en brusfri laserstråle ut från fibern.

Contents

1 Background

This thesis work has been done in the Quantum Information research group at Atomic Physics department at Lund University.
The group is doing research on quantum information using rare earth ions doped in a crystal host. To communicate with the ions a high stability dye laser is used. Because of the extreme performance requirements of the laser the group have to use a high stability laser and modify it with additional stabilization systems.
From 2004-2006 the major part of the research work have been to design and construct a laser with a line width in the order of kHz.

A decision to improve the laser system down to a 10 Hz bandwidth was recently taken. This will increase the control of the system and makes it possible to use ions with even better coherence properties.
It is in this new laser system a fiber noise cancellation system is needed, and the task for this thesis work is to construct such a system.

The laser stabilization system, including the basic working principle of the fiber noise cancellation system was designed by Adam Wiman in a thesis word from 2011[1].
My job was to realize it with real components, build the system and test it.

2 Theory

2.1 Quantum computing

In traditional digital electronics data is represented by bits with value 0 or 1 where 0 and 1 is equivalent with low or high voltage respective.
The bits can be realized by transistors acting as voltage controlled switches when combined can form for example basic logical gates of a handful transistors or advanced processors of billions transistors.

A quantum computing system is based on the same principle where bits control and interact with each other to perform operations.
The big difference is that a quantum bit, qubit, uses quantum properties to be able to be in a superposition of two states. This is not to be confused with analog principle where for example a voltage level could take every value continuously from low to high, but a qubit in superposition can actually be both 0 and 1 at the same time.
By special developed algorithms the quantum system can perform specific calculations mush faster than its counterpart[2].

2.1.1 Rare earth ions as qubits

One important property for the qubits is the coherence time. The coherence is affected when the qubits interact with the surrounding, and the coherence is a prerequisite for the ions to be used as qubits.

Rare earth metals as thorium, praseodymium and europium have a relative long coherence time because of a full valence band. All transitions take place in an inner shell where the electrons are more protected of external disturbances.

The new laser system is constructed for possibility to use Europium ions, Eu^{3+} doped in a non-organic crystal with an optical transition width of 122 Hz. To effetely address the qubits the laser line width should be of an order of 10 Hz.

2.1.2 Hole burning

To "create" specific qubits from the doped crystal a technique called hole burning is used. It's a complex process, but the very basic principle is as following.
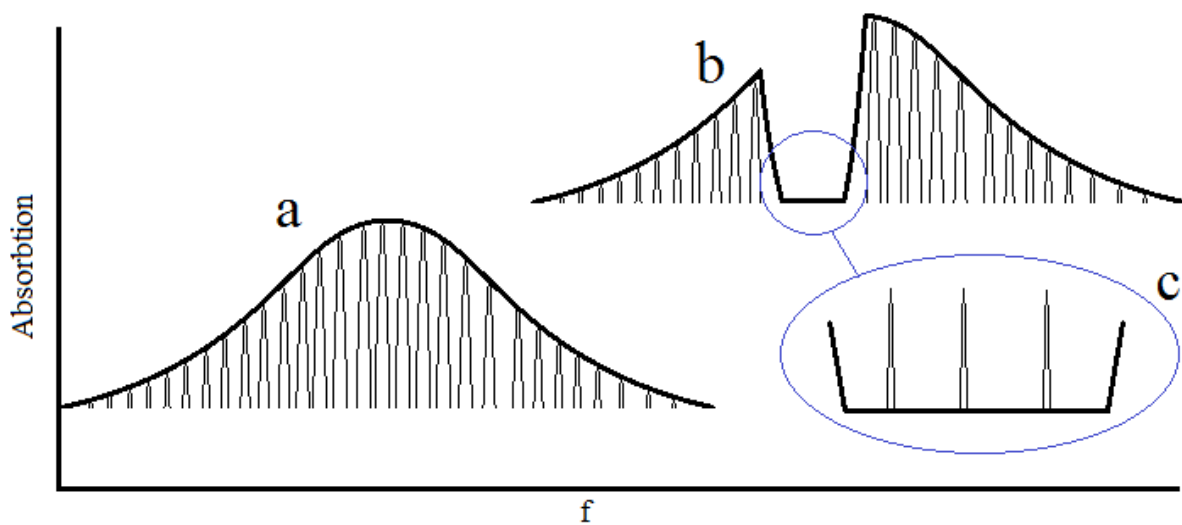
Figure 2. *Hole burning principle.*

a) A crystal is doped with rare earth metal ions creating a wide absorption spectrum.
b) A set of specific laser pulses excite the ions in a small area of the total spectrum where absorption no longer can occur.
c) Another set of laser pulses "puts back" groups of ions in the gap. These groups of ions will be used as the qubits.

2.1.3 Fiber noise

To increase the flexibility optical fibers can be used to transfer the laser from the laser setup to the experiment. This is a big advantage allowing the two, often complex and big, setups to be physically separated.
Due to the mechanic stretch, temperature- and pressure fluctuations in the fiber cable perturbations, called fiber noise, are introduced to the laser beam passing through the fiber cable.
In an article from 1994[3] a 25 m long optical fiber cable introduce a widening of the lasers line width by 300 Hz. This can often be neglected, but in highly frequency stable laser systems this is of big importance.
For a laser frequency stabilized to 10 Hz it's obvious that fiber noise has a major impact.
Unfortunately no time was given to physically measure the phase noise introduced by an optical fiber, but according to the referred article the fiber noise cancellation system is built to cancel noise up to some kHz.

2.2 Fiber noise cancellation

The basic idea of this fiber noise cancellation system is to reflect a part of the laser beam a second time through the fiber, compare it to the original beam and let the beating signal control an AOM regulating the laser beam frequency inverted to the frequency shift in the fiber.
Figure 3 shows the signal flow in a fiber noise cancellation system.
The stabilized laser with frequency f_l is passed through an AOM dividing the beam into the zero and first order of diffraction. The zero-order beam is unaffected by the AOM and is directed to a mirror.
The first order of diffraction beam is shifted the AOM driving frequency, f_{AOM} plus the regulating frequency f_{reg} and is directed into the optical fiber.
The fiber cable introduce some fiber noise, f_n, to the laser beam. After the fiber a beam pick-off reflects approximately 10 % of the beam intensity back again via the fiber, which once more add noise to the beam. The noise added by the both passes through the fiber is considered to be identical due to the speed of light is much faster than the speed of which the fiber noise is changed.
The zero order beam, f_l, and the first order beam double passed through the fiber, $f_l + f_{AOM} + f_{reg} + 2f_n$, coincides in the AOM where once more the zero order diffraction beam is unaffected and the first order diffraction beam is shifted by $f_{AOM} + f_{reg}$.
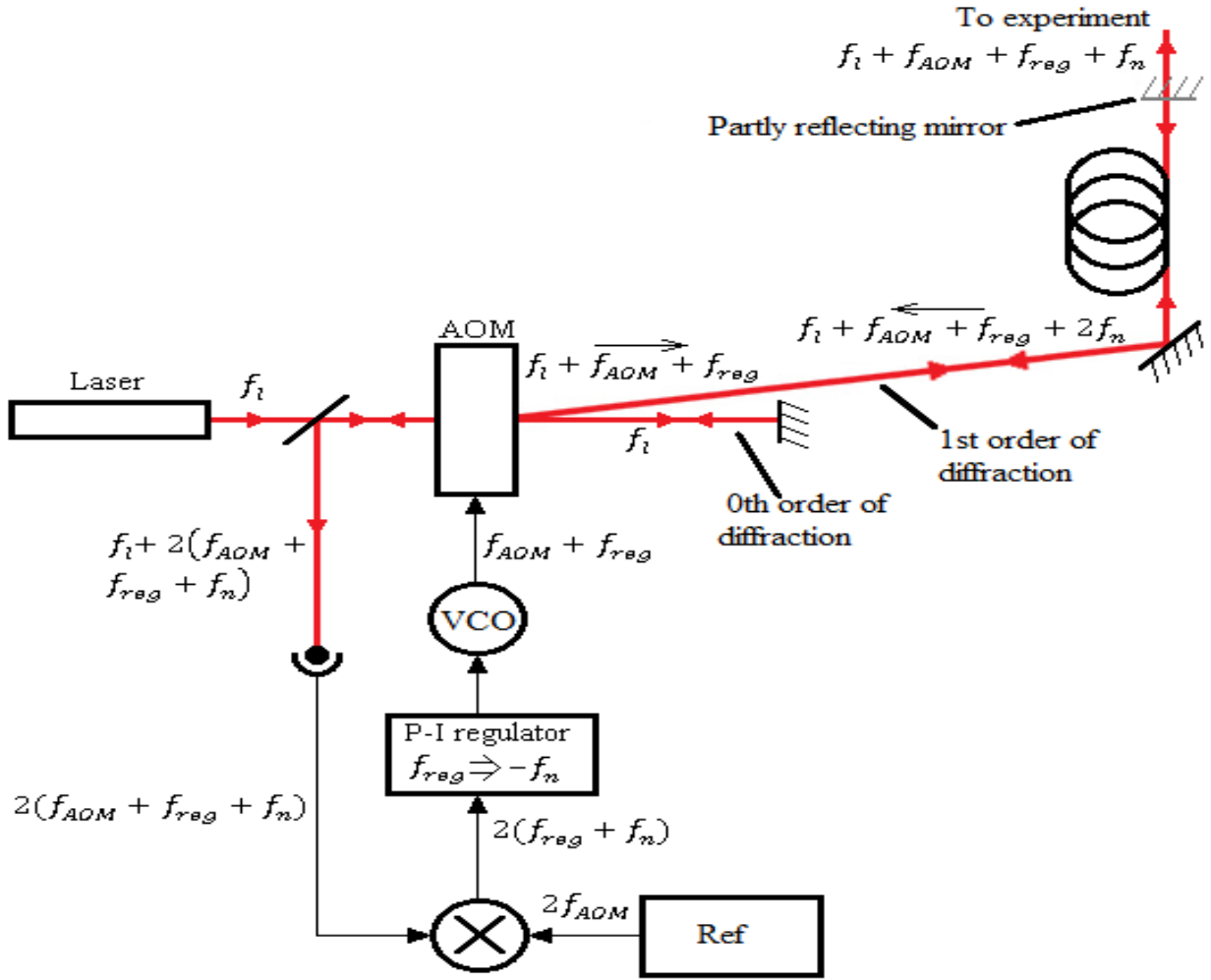
Figure 3. *Basic setup and signals of a fiber noise cancellation system.*

A beam splitter directs the beams to a photo detector where the beating frequency $2(f_{AOM} + f_{reg} + f_n)$ is detected.

The electrical signal is sent to a phase detector where the phase is compared to a high stability reference signal of $2f_{AOM}$. The output from the phase detector is the error signal of the system, $2(f_{reg} + f_n)$, and it is sent to a P-I regulator where the signal is filtered and processed to achieve the controlling signal to the VCO.

This is a phase locking system where the VCO is regulating the phase difference towards zero in the phase detector by attain $f_{reg} = -f_n$.

The output frequency from the system is $f_l + f_{AOM}$. Thus, the system shifts the incoming laser with f_{AOM} but the stability is remained.

One requirement for the fiber noise cancellation system to be effective is that the rate of change of the fiber noise has to be much slower than the regulating speed of the system.

The regulating speed is limited by the time which the laser beam travels two times through the fiber and to the detector, the time for the electronic components to respond and the time for the AOM to change frequency. Because of the great velocity of the light and electric signals the primarily limiting component of the regulating system is the voltage controlled oscillator controlling the AOM.

The fiber noise in other hand is generated by relatively slow temperature, pressure and mechanical changes.

2.2.1 Phase noise and Allan

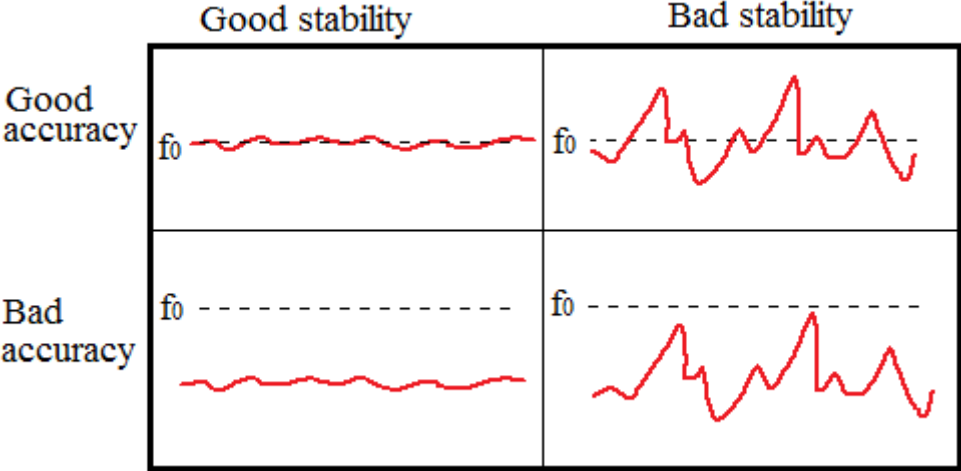Two important figures to characterize an oscillator are accuracy and stability.

Figure 4. *Stability and accuracy.*

Stability is generally measured by the average deviation from a given reference value and the accuracy is a figure of the variation of single measured values. Frequency stability, for example of an oscillator, is often given by phase noise that gives the amount of the relative power located in a bandwidth (generally 1 Hz) for an offset from the center frequency.

By specify the phase noise the frequency noise also is specified due to the relation

$$f(t) = f_0 + \frac{1}{2\pi}\frac{d\varphi(t)}{dt}$$

The Allan variance (named after David W. Allan) is a measure of frequency stability in the time domain and can advantageously be used to compare stability for different oscillators. It is a figure of variance of a number of two-point frequency measurements separated in time by τ.

The mathematic definition of Allan variance without further derivation is

$$\sigma_y^2(\tau) = \frac{1}{2M} \sum_{i=0}^{M-1} \left(y(i+1) - y(i)\right)^2$$

$$M = \frac{T}{\tau} - 1$$

$$y(i) = \frac{\langle f_1(t_0 + i\tau)\rangle_t - f_0}{f_0}$$

where T is the entire measuring interval, τ is the time between two separated frequency measuring and f_0 is the oscillator center frequency.

To transform the phase noise in the frequency domain to Allan variance in the time domain following formula can be used[4].

$$\sigma_y^2(\tau) = \int_0^{f_h} S_y(f) \frac{\sin^4(\pi\tau f)}{(\pi\tau f)^2} df$$

where $S_y(f)$ is the spectral density of fractional frequency fluctuations (phase noise in frequency domain at offset f).
$S_y(f)$ is derived from the linear single sideband noise $L(f)$ by

$$S_y(f) = 2\frac{f^2}{f_0^2} L(f)$$

One of the most important figures when the components to this fiber cancellation system were bought was to not significantly add phase noise to the laser.

2.3 Components

2.3.1 Voltage controlled SAW oscillator

The major difference of a SAW (Surface Acoustic Wave) oscillator from other oscillators is the SAW delay line[5]. In the SAW delay line an input transducer converts the electric signal to an acoustic wave propagating on a quartz substrate surface to the output transducer where it is transformed back to an electric signal. This creates a time delay for signal.
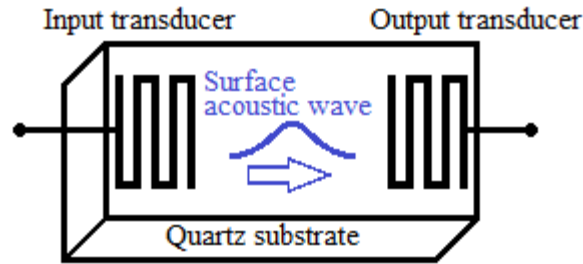
Figure 5. SAW delay line.

A loop amplifier is used, with the SAW delay line as a part of the resonant feedback loop.

The SAW delay line is constructed such that the invers of the time delay is equal to the 3dB bandwidth of the oscillating frequency. By this design the phase shift is 360° over the whole 3dB bandwidth.

To get the amplifier to be unstable and oscillate the loop gain must be greater than unity and the loop phase must be a multiple of 360°. Due to the design of the SAW delay line in the feedback loop the oscillating criteria is only fulfilled at one specific frequency.
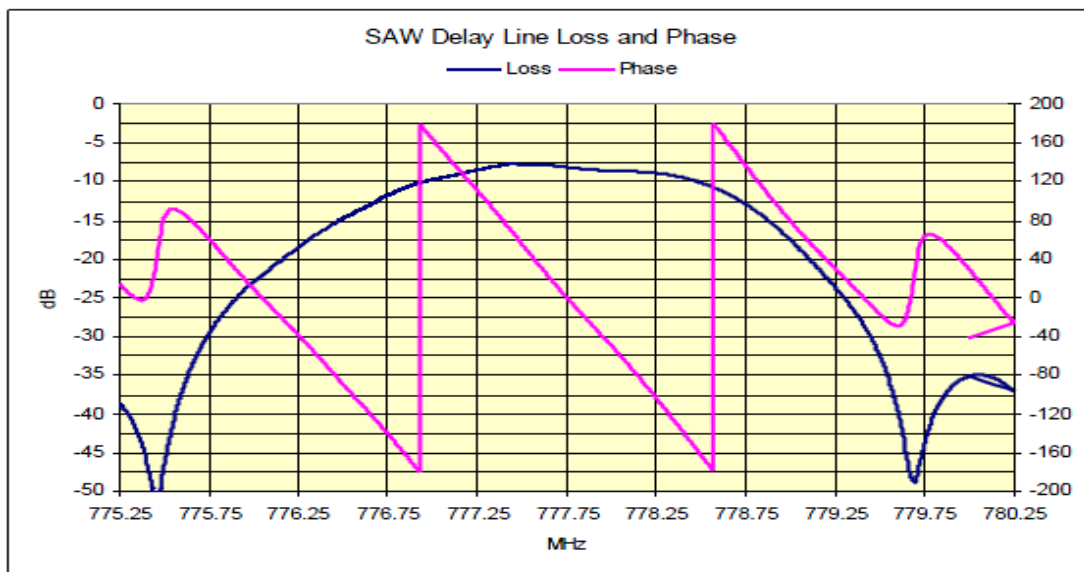

Figure 6. SAW delay line loss and phase (picture from IDT White paper. Voltage Controlled SAW Oscillator (VCSO) Fundamentals (2011).

In a voltage controlled SAW oscillator, VCSO, a voltage controlled phase shifter is added to the feedback loop. The resonant frequency shifts to the frequency where the sum of phase in the SAW delay line and the phase shifter is a multiple of 360°.

This technique gives the VCSO good stability, low phase noise and fast frequency adjustment suitable to be the regulating component in the fiber noise cancellation system.

7

More common oscillators like the voltage controlled crystal oscillator, VCXO, are available for frequencies at 1 GHz with low phase noise and high stability, but the main reason why a VCSO was chosen to this project was the modulation bandwidth that is substantially higher for an VCSO.

2.3.2 Direct digital synthesizer

There are several different ways to synthesize a sinus signal. One technique to obtain high frequency resolution is to use the DDS-technique, direct digital synthesizer.
As the name indicates the DDS technique is not based on analog feedback as the phase locked loop synthesizer, but on a digital tuning word clocked by a system clock.
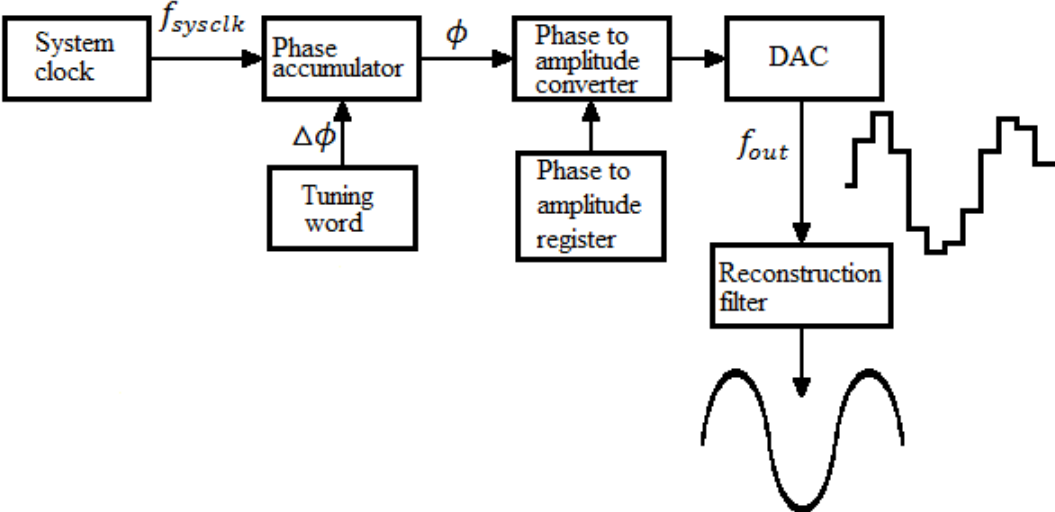

Figure 7. *DDS building block schematic.*

A digital tuning word determines the phase $\Delta\phi$ added to the phase accumulator every system clock cycle to obtain the desired frequency f_{out}.

The digital phase signal from the phase accumulator to the phase to amplitude converter for each n system clock step is

$$\emptyset_{n+1} = \emptyset_n + \Delta\emptyset$$

When the phase value from the phase accumulator excess the value of 2π, 2π is subtracted from the phase value preventing the value to increase uncontrolled.

The output frequency depends on two parameters; the system clock frequency and the tuning word.

$$f_{out} = \frac{f_{sysclk} \cdot \Delta\emptyset}{2\pi}$$

The number of bits in the tuning word determines the degree of frequency resolution in the DDS, halving the minimum addable phase in each clock cycle for every extra bit.

$$resolution = \frac{f_{sysclk}}{2^N}$$

where N is the number of bits in the tuning word and is typically $24 - 28$ bits long which allows down to micro hertz resolution.

A phase to amplitude converter uses a register to convert the phase to amplitude before the digital to analog converter, DAC, synthesize the analog signal f_{out}. The signal out from the DAC has a step shape with f_{sysclk}^{-1} step time. To get a clean sinus signal out a reconstruction filter is applied reducing the harmonic frequencies $n \cdot f_{sysclk} \pm f_{out}$ where n is order of harmonic.

One advantage of a DDS is that the tuning word doesn't have to be constant. It can be changed to immediate change the output frequency without any disruption in the output signal.
The tuning word is often controlled by a programmable microprocessor, but in this thesis work the tuning word is held constant and instead the VCSO system clock is varied to regulate the output frequency.

The VCSO center frequency is static but has the ability to be voltage controlled. The DDS on the other hand has an output adjustable over a wide range of frequencies but requires reprograming of the microprocessor to change frequency.
By using a VCSO to clock the DDS the advantages of the both is obtained to get a voltage controlled oscillator with adjustable center frequency.

2.3.3 Acousto-optic modulator

To shift the frequency of a laser beam an acousto-optic modulator, AOM, can be used. Longitudinal acoustic waves in a transparent crystal create a grating where high and low sound pressure creates a change in the index of refraction which deflects part of the beam.

An important difference from a stationary grating is that the acoustic grating propagates through the crystal with the speed of sound causing a Doppler shift in the diffracted laser beams.
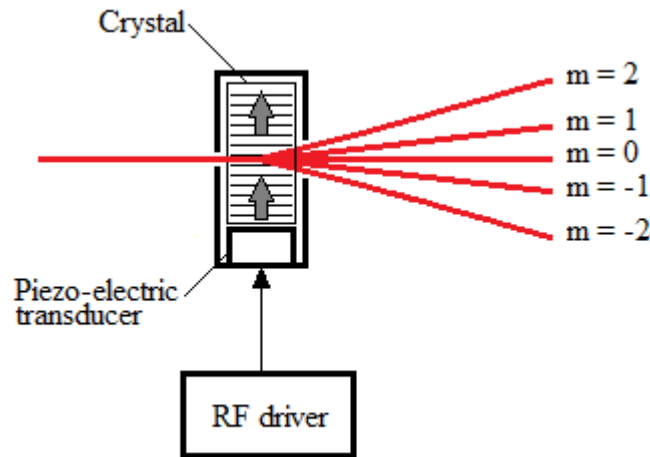
Figure 8. AOM.

Braggs law determines the relationship between wavelength at incoming wave λ, distance between grating lines d and angle of diffracted beams Θ at order m.

$$m\lambda = 2d \sin \Theta$$

The crystal can be made of for example fused silica, Quartz, tellurium dioxide (TeO2) or lead molybdate (PbMoO$_4$).

The AOM is driven by a RF frequency, f_{RF}, in the order of 100 MHz which gives the distance between the acoustic wave grids

$$d = \frac{v_{crystal}}{f_{RF}}$$

where the speed of sound in the crystal is of order $5 \cdot 10^3$ m/s, but vary for different crystals.

Due to the velocity of the acoustic grid the frequency of the incoming beam is Doppler shifted by

$$\Delta f = m \cdot f_{RF}$$

and the zero order beam frequency is therefore unaffected.

Depending on the choice of diffracted beam both a positive and negative frequency shift can achieved.
The modulation bandwidth is related to the time it takes for the acoustic wave in the crystal to pass the laser beam and can be increased by decreasing the laser beam diameter.

The AOM can also be used for amplitude modulation, but this is not covered here.

2.3.4 Rubidium reference

A noise free laser is not enough to be able to make quantum experiments. The laser needs to have long time stability as well to be able to repeatedly address the same qubit at separated times.

Some of the most accurate frequency standard is based on transitions in atoms. The SI standard for one second is for example based on a hyper-fine transition in Cs-133.
Both commercial cesium and rubidium references are available. The cesium reference has a typical accuracy at $\sim 1 \cdot 10^{-12}$ and a rubidium reference an order higher.
Because of the high price of cesium references (several hundreds of thousand SEK) a rubidium reference was purchased for use in this system.

2.4 Radius of curvature.

The fiber noise cancellation system and the test system contain two photo detectors where the beating signal of two laser beams is detected on each detector.
Because of the radius of curvature in a laser beam is changing over distance, two laser beams from a single source that have been travelled different distances have different radius of curvature. If the radius of curvature difference is big at two beams on a detector they can cause destructive interference that make the signal hard to detect.

There is no parallel laser beams. The beam radius, W, is always increased for increased distance, z, from the beam waist, $z = 0$, where there is a minimum beam radius, W_0.
The beam front radius, R, is also changed with distance. At $z = 0$ the wave front is parallel and $R = \infty$. For increasing z, R decreases to a minimum at $z = z_0$ and then increase again for increased z.
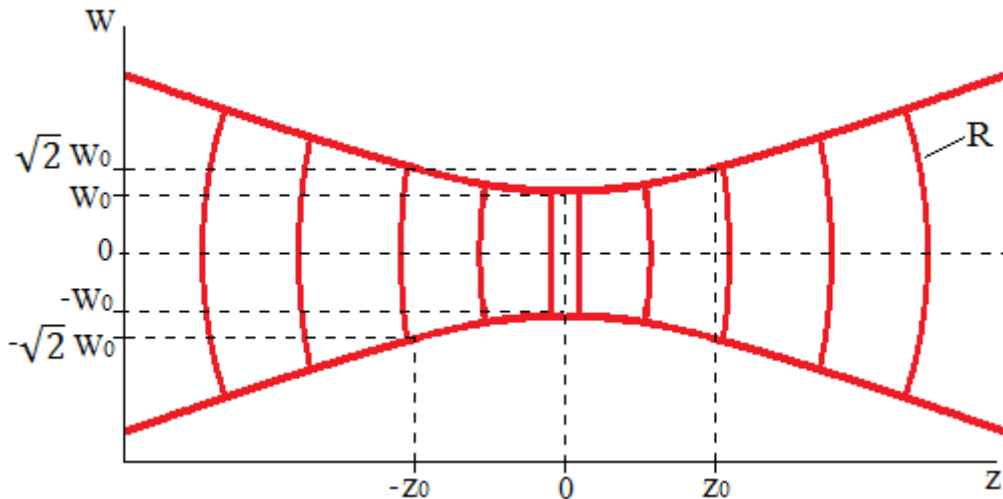Three equations for the relationship between the optical parameters are shown below.

Figure 9. Gaussian laser beam.

$$W = W_o \sqrt{1 + \left(\frac{z}{z_0}\right)^2}$$

$$R = z \left[1 + \left(\frac{z_0}{z}\right)^2\right]$$

$$W_0 = \sqrt{\frac{\lambda z_0}{\pi}}$$

An illustration of wavefronts of two laser beams from the same source but with different optical way from the source to detector is shown in *Figure 10*.
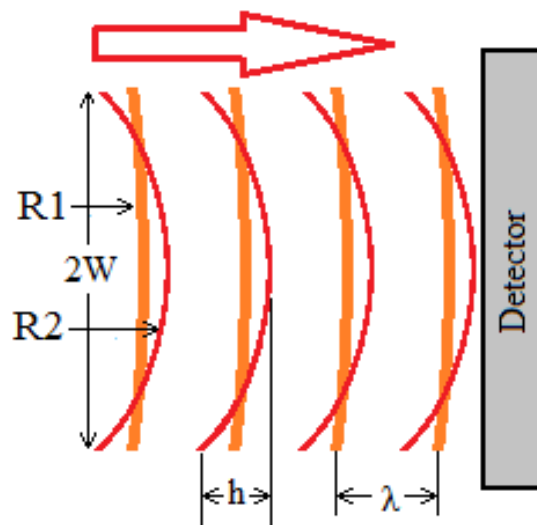

Figure 10. Wavefronts from two beams with different optical length on a detector.

If the difference in wavefront radius of the two beams is significant the beating signal can be hard to detect due to destructive interference.

12

The difference in length of two beams from a single source to a single detector that can be used before destructive interference starts to occur can be calculated by calculate the bending distance, h, which is derived from formula for circle segment.

$$h = R - \sqrt{R^2 - W^2} = R\left(1 - \sqrt{1 - \left(\frac{W}{R}\right)^2}\right)$$

The maximum value for $\frac{W}{R}$ saturate for big z at $\frac{\lambda}{W_0\pi}$.

Because $\left(\frac{W}{R}\right)^2 \ll 1$ (except for extremely small W_0) approximation $1 - \sqrt{1-a} \approx \frac{a}{2}$ can be used to get

$$h \approx \frac{1}{2}\frac{W^2}{R} = \frac{1}{2}\frac{\left(W_0\sqrt{1 + \left(\frac{z}{z_0}\right)^2}\right)^2}{z\left[1 + \left(\frac{z_0}{z}\right)^2\right]} = \frac{1}{2}\left(\frac{W_0}{z_0}\right)^2 z = \frac{1}{2}\left(\frac{\lambda}{\pi W_0}\right)^2 z$$

Now it's easy to determine the maximum difference in distance for the two laser beams before critical wavefront bending occur.

For more convenience a limit can be set for parameter h and a graph for optical length and beam waist can be plotted.
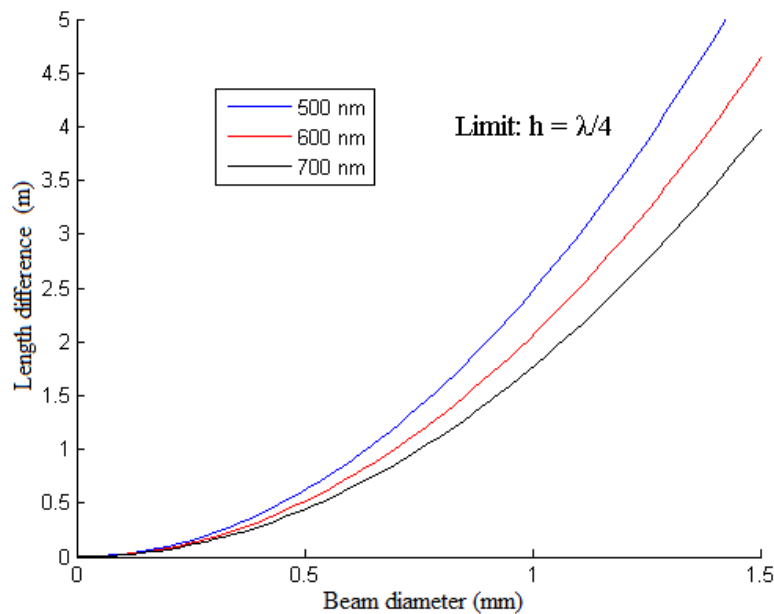
Figure 11. Maximum length difference relative to beam diameter.

This thesis work contains just a handful of optical components and could have been constructed to get an optical length of approximately $10 - 20$ cm if it wasn't for the AOMs. Because the small diffraction angle ($\sim mrad$) it is

13

difficult for small distances to separate the zero and first order diffracted beams used in the fiber noise system.

With a special half circle shaped mirror which is reflective all the way to the edge the beams is separated successfully at 30 cm. The difference in optical length for the two beams are estimated to less than 1 m. *Figure 11* then shows that the minimum beam diameter is approximately 0.7 mm for a 622 nm laser.

3 Building the system

3.1 Schematics

Schematic for the fiber noise cancellation system is shown in *Figure 12*. Components over the green dashed line is only for control measuring, not a part of the fiber noise cancellation system itself.
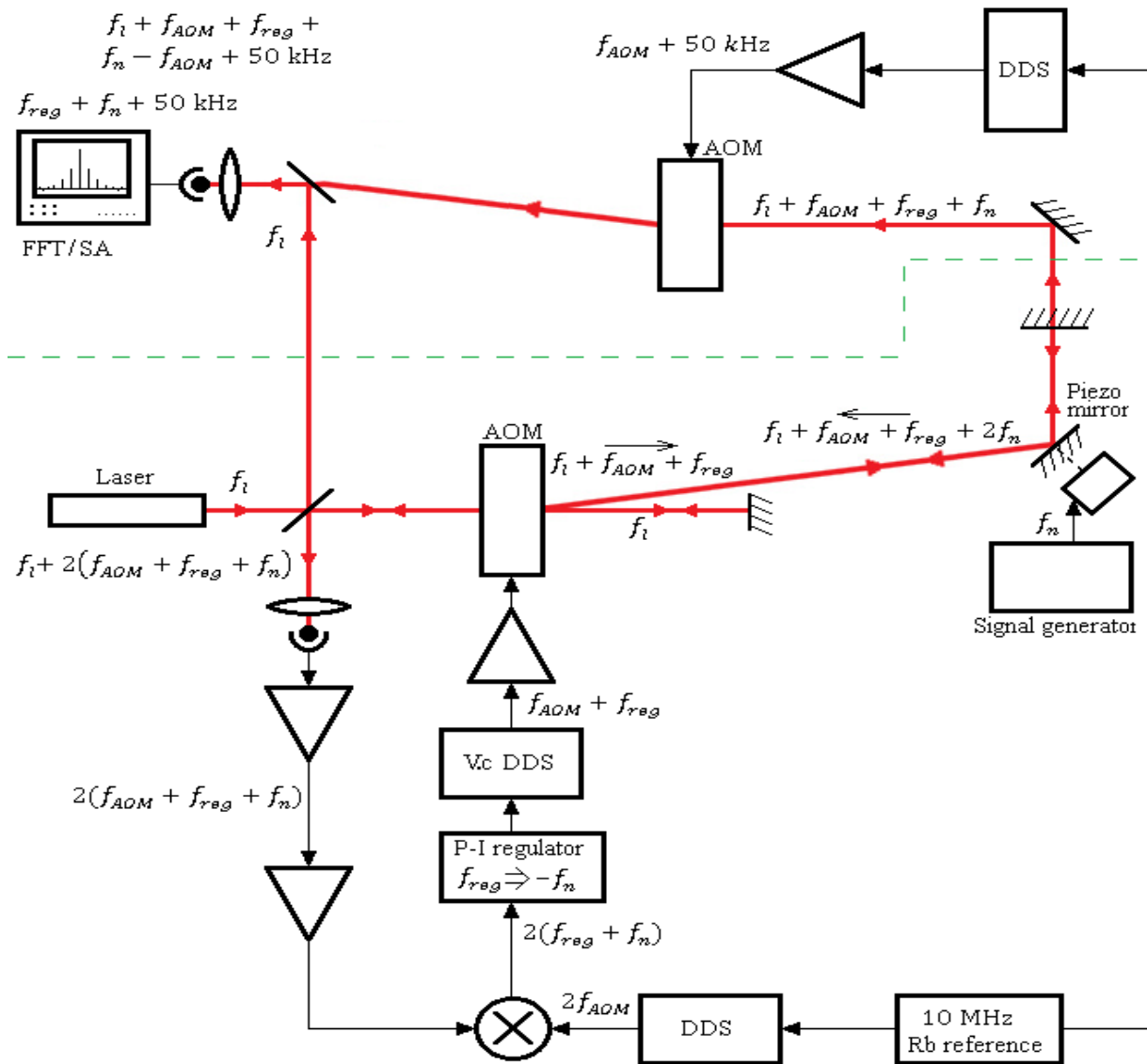
Figure 12. *The constructed fiber noise cancellation system.*

Components in the system not described further in this thesis work are:
- Frequency locked He-Ne laser with $\lambda = 632.8$ nm ($f_l \approx 5 \cdot 10^{14}$ Hz) from Spectra physics.
- Isomet AOM 1205C-2.
- Physik Instrument Piezo actuator and LVPZT-amplifier.

- SRS DS345 signal generator
- Home made high speed photo detector. This detector did unfortunately not work properly, so it was replaced by another home made detector.
- Thorlabs B2200 photo detector.
- Mini-circuits RPD-2 Phase detector.
- Novatach DDS 425A.
- Novatech DDS 409B (10 MHz reference input option).
- Lecroy Wave Runner HRO 66Zi oscilloscope with FFT/spectrum analyzer software.

The control measuring part (above the green dashed line) is used to, by a second AOM, shift back the laser to the original frequency, but with a 50 kHz offset $f_l + f_{AOM} + f_{reg} + f_n - f_{AOM} + 50$ kHz.

This beam is mixed with the original beam in a beam splitter and directed to a photo detector detecting the beating signal $f_{reg} + f_n + 50$ kHz.

When the fiber noise cancellation system is working properly $f_{reg} = -f_n$ and the only signal measured by the spectrum analyzer is the 50 kHz offset signal.

No fiber is used in this setup. Instead a mirror attached to a piezo crystal is used to simulate fiber noise. The piezo crystal is connected to a signal generator for controlled amplitude and frequency fiber noise simulation f_n.

To generate an accurate and stable reference frequency ($2f_{AOM}$) to be connected to the phase detector a DDS is used disciplined by a 10 MHz Rubidium reference. This Rubidium reference is also used to discipline the AOM used in the control measuring part.

3.2 Voltage controlled DDS

The central component of this fiber noise cancellation system is the voltage controlled DDS system, and it is the component that required the most time to construct.

Many solutions were investigated to use as this regulating component.

Oscillator requirements:
- A sinus wave oscillator with center frequency of 70 MHz, but should be able to work with other output center frequencies as well in other applications.
- Low phase noise
- Modulation bandwidth of > 20 kHz
- Frequency modulation range of > 20 kHz with 1 Hz resolution

The modulation bandwidth and the modulation range requirements were set to with margin exceed the maximum frequency component in the induced fiber noise.

A good signal generator with external modulation will meet these specifications, but due to the high price it was rejected.
Many different VCO and VCXO solutions where investigated, but it was hard to find any with modulation bandwidth over 10 kHz.
A VCSO have all the desired properties from the list above except it was hard to find a VCSO operating at 70 MHz. The solution was to use a high frequency VCSO as system clock in a DDS generating the desired frequency.
By this combination the center frequency can be set to a wide range of frequencies by changing the DDS setting, but still the frequency rapidly can be voltage controlled by the VCSO.

The DDS used in this system is AD9912 from www.analog.com. It is a 9×9 mm chip, but can be bought as an evaluation board where the chip are soldered to a circuit board together with a USB port and a USB controller, SMA connectors for power supply, system clock input, multiple output options with or without a reconstruction filter and prepared bays to solder an oscillator or crystal to use instead of external system clock.
By the USB connection most of the DDS settings can be controlled by the provided software.
The DDS has 48 bit$s$ tuning word, maximum system clock frequency of 1 GHz and max output frequency range of $10 \text{ MHz} - 0.4 \cdot f_{sysclk}$.
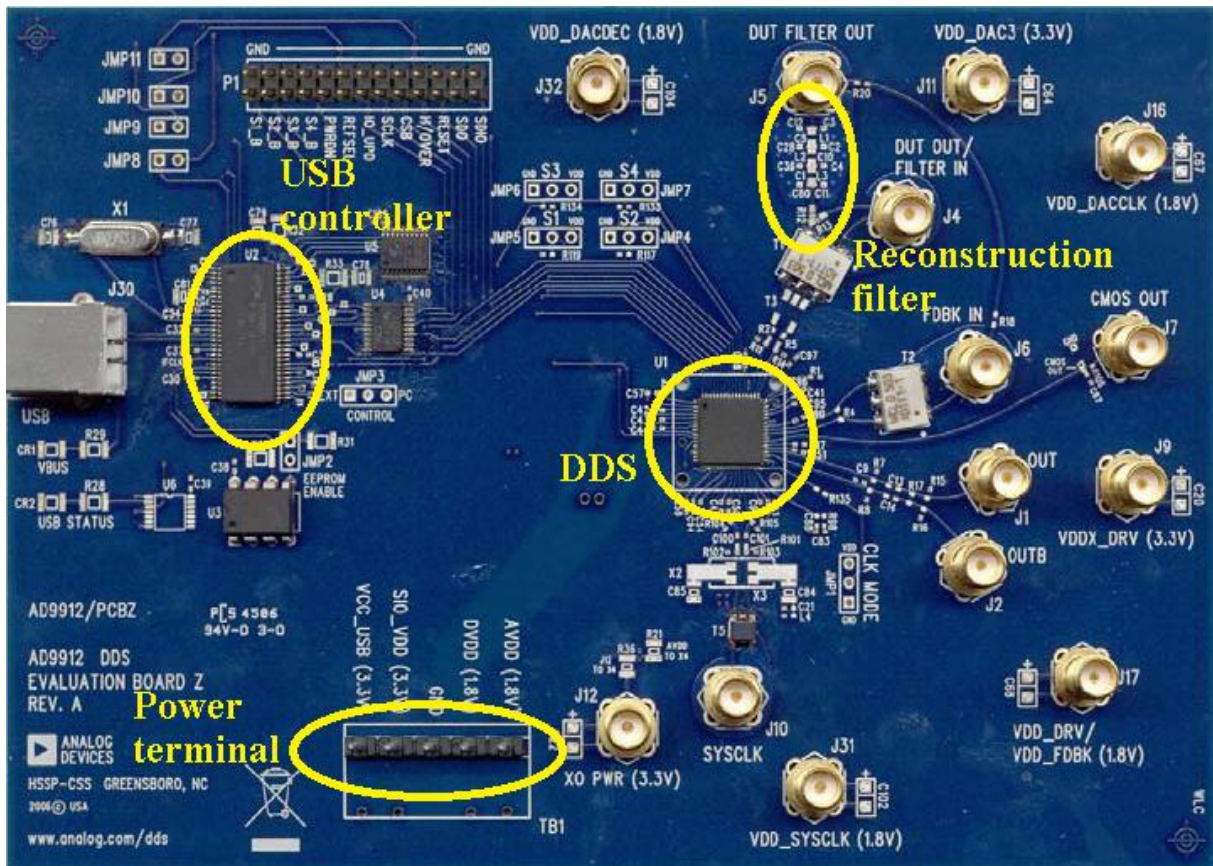A $7th$ order 400 MHz reconstruction filter is integrated.

Figure 13. *DDS evaloution board.*

The work that had to be done to get the voltage controlled DDS "ready to go" was:

- Solder the VCSO and adjust the termination resistors.
- Power supply.
- Adjust reconstruction filter.
- Build in DDS card and power supply card in a box with connections.

3.2.1 VCSO

Used VCSO: Crystek CVS575 622.08 MHz.
The DDS can handle a system clock frequency of 1 GHz. According to Nyquist theorem the sampling frequency must be at least doubled to the discrete sampled signal. This is because the sideband frequencies are
$n \cdot f_{sysclk} \pm f_{out}$ Hz.
If $f_{sysclk} = 2f_{out}$ the lower of the first order sidebands, $f_{sysclk} - f_{out}$, coinciding with f_{out}. The DDS manufacture has sat a limit for the output frequency to $f_{out} < 0.4 \cdot f_{sysclk}$.

18

To get a clean sinus output the overtones has to be filtered out. For higher system clock frequency the frequency distance between the wanted output signal and the overtones is increased making the filtering less complicated.

It proved harder than expected to achieve the 1 GHz VCSO, but one VCSO at 622.08 MHz from Crystek with a modulation bandwidth of 500 kHz was found and purchased.
According to the VCSO data sheet the tuning sensitivity is 275 ppm/V and the control voltage level is $0 - 3.3$ V. This makes it theoretically possible to change the VCSO frequency

$$275 \, \text{ppm/V} \cdot 3.3 \, \text{V} \cdot 622.08 \, \text{MHz} \approx 565 \, \text{kHz}$$

Because the synthesized output frequency from the DDS is proportional to the system clock frequency the output frequency of 70 MHz can be modulated by

$$275 \, \text{ppm/V} \cdot 3.3 \, \text{V} \cdot 70 \, \text{MHz} \approx 64 \, \text{kHz}$$

which fulfills the requirements.

A measurement of the VCSO shows a non-linear behavior for the control voltage making the effective frequency range significantly smaller compared to the theoretical figure. Still the VCSO can be controlled ± 15 kHz which is sufficient for the fiber noise cancellation purpose.
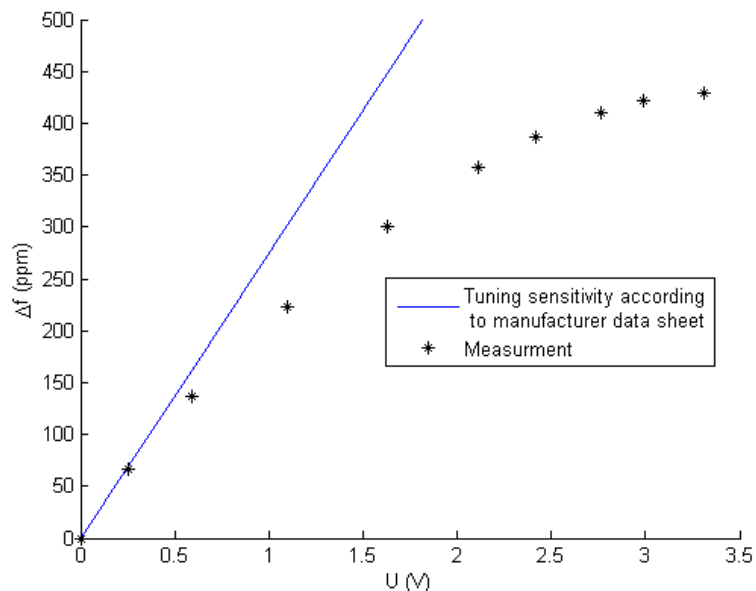
Figure 14. V-f characteristics for the VCSO.

There are three different ways to clock the DDS on the evolution board; connect an external clock signal through the SMA connection or solder a crystal or an oscillator to the prepared bays.

The DDS has an internal PLL doubler and a PLL multiplier for the system clock making it possible to use a clock source of only a few MHz.
When using the 622 MHz VCSO the system clock PLL doubler and multiplier has to be bypassed not to exceed the clock frequency limit of 1 GHz.

Small physical modifications have to be done to the evaluation board for using the VCSO.
Two long unused lines in the path from the VCSO to the DDS input has to be cut off preventing them to act like antennas picking up noise adding to the VCSO clock source. In the extension of the same lines a transformer is connected. This may also affect the performance and is good to disconnect as precaution.

According to the evaluation board data sheet a 10 nF decoupling capacitor has to be soldered to decouple the power supply for the VCSO. The board has a prepared bay for a standard size component 0402 for this.

The termination of the VCSO is important for the performance. The used VCSO has a LVPECL (Low-Voltage Positive Emitter-Coupled Logic) differential output with $U_{low} = 1.6$ V and $U_{high} = 1.3$ V. Resistors $R101 - R103$ have to be replaced by new ones to create a 50 Ω load to the VCSO (100 Ω differential). $R102$ and $R103$ are needed to create a DC path to ground and are recommended to be at $140 - 220$ Ω[6].
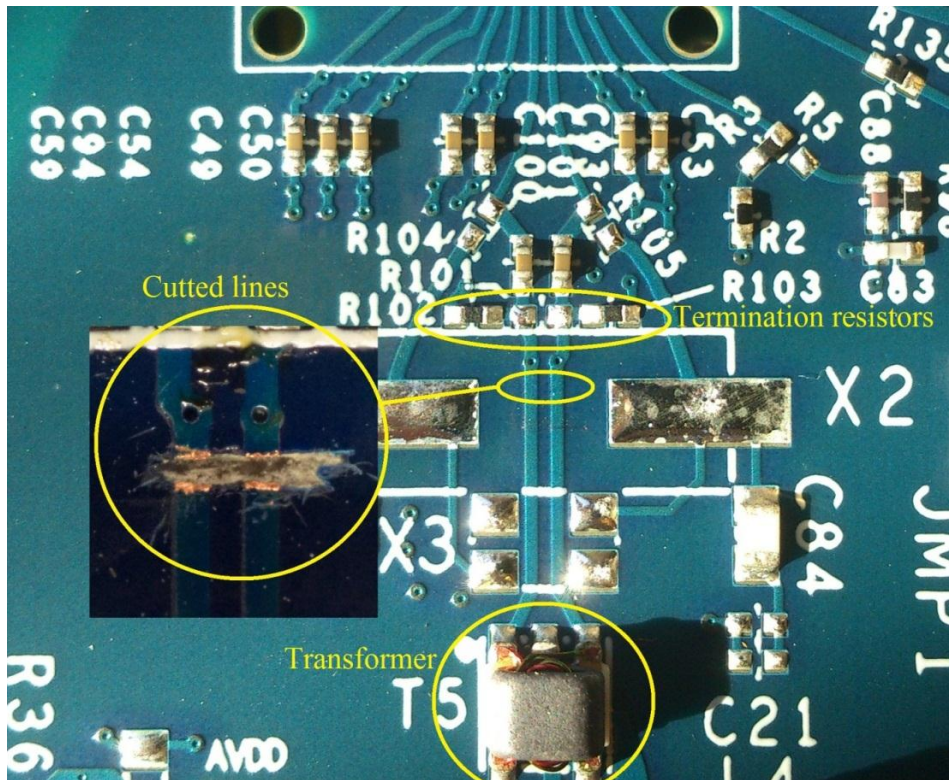Resistor values of 180 Ω for $R102$ and $R103$ is used, and resistor $R101$ is chosen so that the total differential resistance becomes 100 Ω.

$$R101 = \left(\frac{1}{100 \ \Omega} - \frac{1}{(R102 + R103)} \right)^{-1} \approx 140 \ \Omega$$
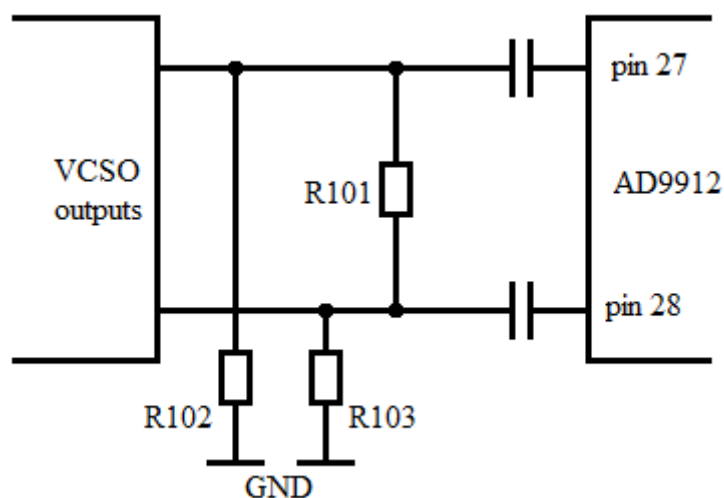


Figure 15. Termination schematic.

Figure 16. *The three termination resistors (the middle one is not yet soldered), a zoom in at the cut lines and the unused transformer.*

The prepared oscillator bay on the evaluation board has connections for power supply, ground and output signals, but two additional signal must be connected to the VCSO; 3.3 V to the enable/disable pin making the VCSO active and the voltage signal used to control the frequency shift.

Wires were soldered connecting the enable/disable and the power supply pins together, and from the voltage control pin to an electric screw terminal.

The termination resistors and decoupling capacitor are of standard size 0402 (0.039 × 0.02 in, or 1 × 0.5 mm), and the contacts on the board for the VCSO are almost completely covered by the VCSO itself, which make them difficult to solder manually. With a microscope, a sharp soldering iron, steady fingers and a good temper the components finally came to right place.
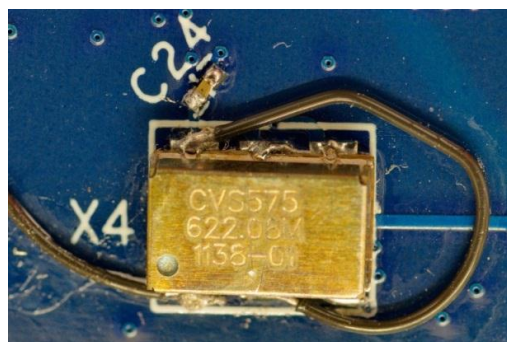

Figure 17. *VCSO with decoupling capacitor and wires for enabling and frequency control.*

21

3.2.2 Power supply

Three separated power cards are used to supply the DDS evaluation board. The cards is called "Breadboard Power Supply Stick 3.3V/1.8V" model number PRT-10934 and was purchased from www.funspark.com. The board requires stable voltage source of 1.8 and 3.3 V distributed to supply different parts of the board as the USB controller, oscillator and different analog and digital parts of the DDS (the DDS chip itself has 20 pins for power supply).
To get the best performance of the DDS the digital and analog power supplies should be separated by different power sources. One reason for this is that the distortion, for example overtones, has different characteristics for analog and digital signals. The very sharp edges in a digital signal causes high frequency noise that needs to be isolated from the analog signals.

Separating all different power supplies to get the ultimate performance is practically complicated and expensive. The DDS evaluation board data sheet provides recommendations which power supplies are to be grouped together, separated by a ferrite bead or separated by different power regulator.
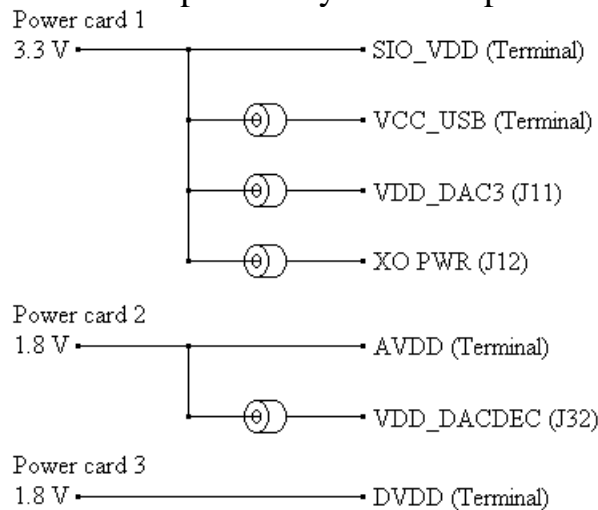
Figure 18. Power distribution.

The typical current consumptions for the DDS evaluation board are specified in the data sheet with the exception of the VCC_USB connection.
VCC_USB current consumption is calculated by adding the individual components current consumption from their data sheets. Components supplied from that power connection is one USB microcontroller, one EEPROM, two buffer/driver and one Schmitt trigger.

Supply	Typical current consumption (mA)
Power card 1	
SIO_VDD	2
VCC_USB	51
VDD_DAC3	26
XO PWR	82
Total	161
Power card 2	
AVDD	113
VDD_DACDEC	40
Total	153
Power card 3	
DVDD	205
Total card 3	205
Total	519

The figures given in the data sheets are typical values and can varying dependent on the operation. For example digital circuits consume very little power when they are static and consume a bigger current for a very short time at the moment of switching between 0 and 1. Some parts of the evaluation board are disabled, as the CMOS output stage and system clock PLL multiplier and doubler making the actual current consumption to be lower than the typed.

The power cards used to supply the evaluation board can by a switch be set to deliver a regulated 1.8 or 3.3 V. They have solderable connections for supply power in and regulated power out.
No data sheet for max current delivery was unfortunately available. The regulating component on the cards, voltage regulator LD1117, has a type current of 950 mA, so to be able to get 205 mA out from the card seems reasonable.
A non-scientific test was done with the power cards using a power source, a current meter, some loading resistors and a human temperature measuring device (finger). The power card was loaded to deliver 400 mA for several minutes, both at 1.8 V and for 3.3 V without getting significantly hot.
For output current of 680 mA for 30 s the voltage regulating circuit was getting hot enough to burn the finger. The conclusion was taken that the power cards would deliver the 205 mA current to the DDS evaluation board with margin.

The operating current consumption of the voltage controlled DDS system was measured to 362 mA which gives a total effect of 2.172 W for a 6 V supply voltage.

According to the power card data sheet the supply voltage could be between $4 - 9$ V. Measuring the output frequency when varying the power supply voltage shows that for supply voltage below 4.7 V the frequency starts to be affected. What causes this frequency shift is not investigated further, but gives important knowledge how to supply the power cards.
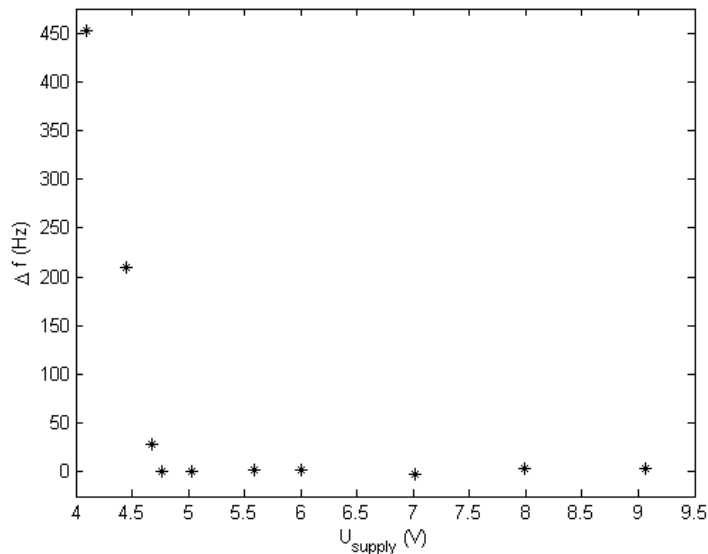
Figure 19. Voltage controlled DDS system. Supply voltage vs. frequency affect.

3.2.3 Reconstruction filter

The filter was bought from www.digikey.se and has model number Crystek CLPFL-0300.

On the evaluation board a reconstruction filter is integrated. The filter is a 7th order elliptical low-pass filter with a cutoff frequency of 400 MHz.

The main purpose of the filter is to attenuate the sidebands to get a clean sinus signal out from the voltage controlled DDS system. The sideband with lowest frequency occur at

$$f_{sysclk} - f_{out} = 622 \text{ MHz} - 70 \text{ MHz} = 552 \text{ MHz}$$

which is only reduced 20 dB by the integrated filter.

To get rid of as much sidebands as possible a filter with a low frequency cutoff should be used, but not so low that the 70 MHz output signal is affected by negative gain or phase shift.

It's possible to modulate the evaluation board by changing the filter components for new ones to

Figure 20. External reconstruction filter.

24

obtain the desired cutoff frequency. This requires some calculations and difficult soldering work, so an external filter with SMA connections is purchased and connected in series with the integrated filter.

The external filter is a 300 MHz low pass of 7th order from Crystek.

By connecting the two filters in series the effective equivalent filter is of 14th order with attenuation of 280 dB/dec for frequencies over 400 MHz and will attenuate the 552 MHz sideband with 57 dB without affecting the phase or gain on the 70 MHz output signal.
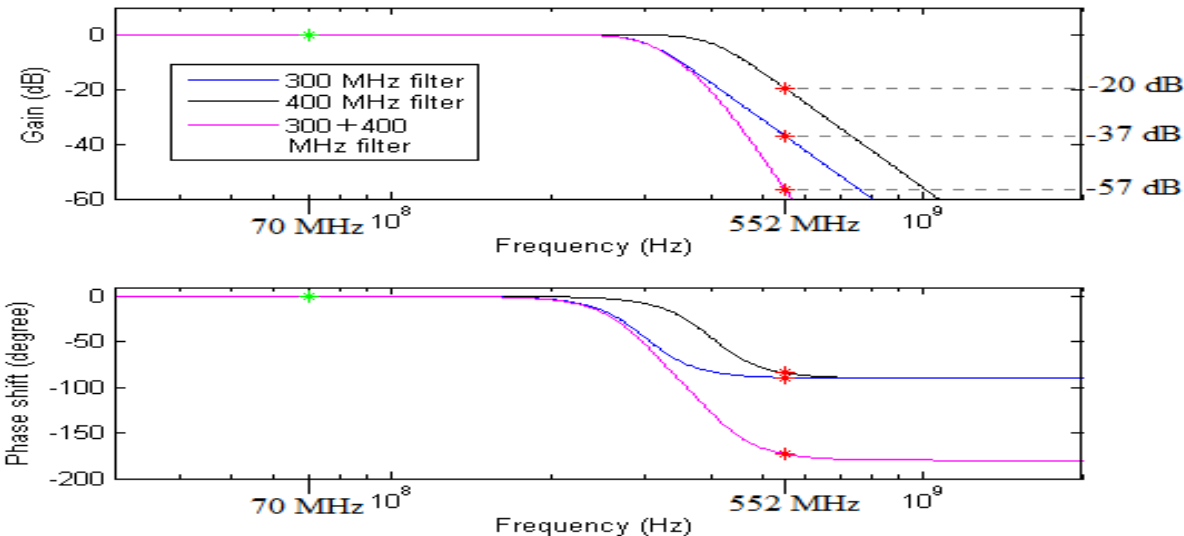

Figure 21. *Filter frequency response.*

3.2.4 Box

An aluminum box is used to encapsulate the evaluation board and power cards. It also gives some electromagnetic protection preventing noise to be picked up by unshielded cables and circuit board wires.

The box is a Hammond 1550 WJBK.

The evaluation board is mounted in the box by plastic circuit board holders. Holes have to be drilled in the circuit board for attachment. The evaluation board documentation contains information about the four different layers in the circuit board so that the holes can be drilled without causing any damage to the circuit board. Two of the layers are ground and power layer which extends over almost the whole card area. Because the holders consist of isolating plastic using them is not a risk for shortening the layers. Big caution must be taken so that no swarfs are left after drilling shortening the layers.

The power cards have no place for drilling holes. Instead they are glued to a metal plate attached by the circuit board holders. A BNC female connection attached to the box is used for power supply, the USB cable, the SMA control voltage cable and the SMA output cable are passed through grooves filed between the box and the top protected by rubber bushings.

3.3 Protection circuits amp

All three amplifiers are purchased from www.minicircuits.com. Two of them is identical low-noise amplifiers with model number ZX60-33LN+ and one is a high power amplifier with mounted cooling fins and fan, model number ZHL-03-5WF.

Input and output connections are of SMA type, but the power supply connectors needs to be soldered. A small console with banana plugs, decoupling capacitors and TVS (transient voltage suppression) diode is constructed.
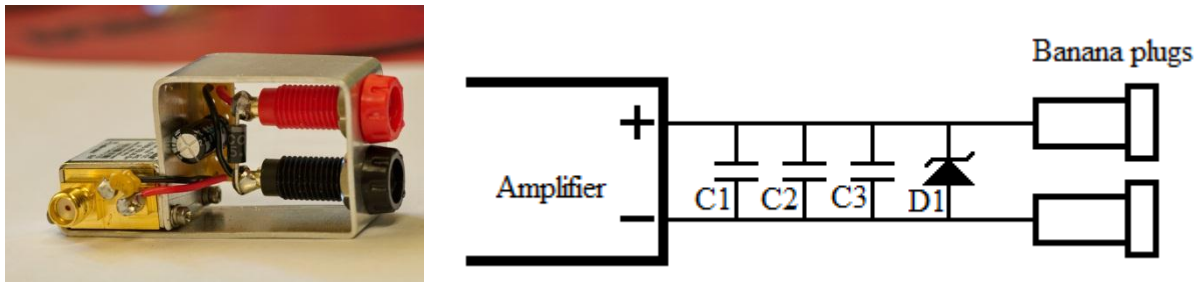

Figure 22. *Colsole and amplifier power supply circuit.*

To prevent damage of the amplifiers the TVS diode is connected parallel to the power supply connections protecting the amplifier against harmful high voltage and reversed power supply.

If the power supply is mistakenly reversed the diode will act almost as a shortening drawing all the current preventing reversed voltage polarity to the amplifier.

The diode has a defined breakdown voltage where it starts to conduct, and it is chosen so that no current goes through the diode for normal operation voltage. When the breakdown voltage is exceeded the diode starts to conduct preventing harmful the voltage to increase further.
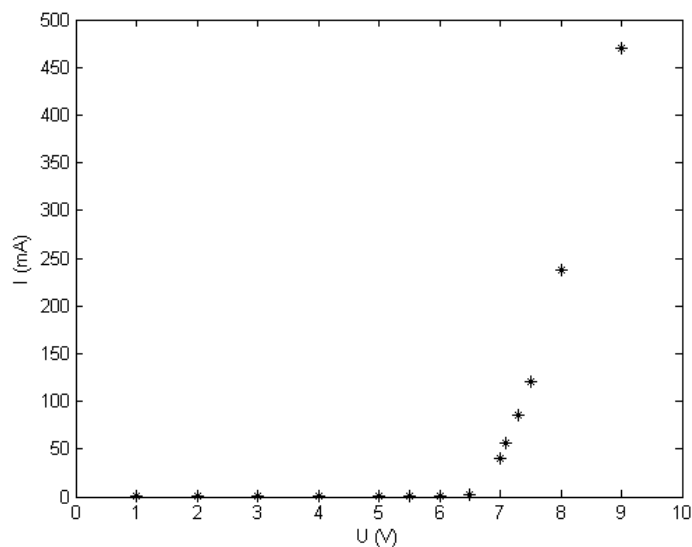
Figure 23. *I-U characteristics of the 5 V TVS-diode used in the low-noise amplifiers.*

To be able to draw a big current away from the protected device the diodes are of high power type. To protect the amplifiers in this thesis work diodes with a label effect of 500 W is used, and because of the maximum power outputs from the used power supplies are 90 W the diodes will handle all that power with margin.

The decoupling capacitors have two main purposes.
One is to help the power supply deliver a stable dc voltage to the amplifier. Due to the high frequency and high power the slew rate, $\frac{\Delta V}{\Delta t}$, is very high and the power consumption in the amplifier is therefor changed rapidly. The capacitor acts like a power backup for quick power delivery.
The other purpose is to filter out noise induced in cables and from power supply. High frequency noise will go through the capacitors instead of entering the amplifier through the power supply preventing to affect the output signal from the amplifier.

If capacitors are parallel connected the total equivalent capacitance is the same as the sum of the individual capacitors. So why not use one single big capacitor instead of several small ones? The answer is parasitic inductance.
There are no such components as an ideal capacitor. A capacitor has always parasitic components such as inductance and resistance.

The parasitic resistance R_p, is usually much smaller than 1 Ω and is not very affected by the frequency, but the parasitic inductance, L_p, has a big influence at the total impedance for high frequencies.
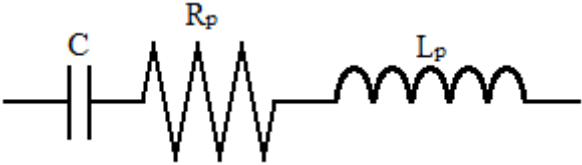

Figure 24. *Simplified equivalent circuit of a capacitor.*

$$Z = \frac{1}{j\omega C} + R_p + j\omega L_p$$

The parasitic inductance figures are seldom to be found in the manufacturer datasheets so it has to be measured with a network analyzer for precise decoupling matching.

To be able to simulate the frequency response of the decoupling capacitors the parasitic inductances are approximated by using the formula for inductance in straight wire conductors[7].

$$L_p = 2l\left(\ln\frac{4l}{d} - 1\right)$$

By calculating the parasitic inductances by this formula the basic idea for using several different decoupling capacitors is shown.
According to the formula the inductance is increases with length, l, so to achieve low inductance it is important to keep the conductors short. This is the reason why the small capacitors are soldered directly to the power supply pins at the amplifiers.

Ohms law gives that when two capacitors with parasitic components are parallel connected, the equivalent capacitance is increased, and at the same time the parasitic resistance and inductance in reduced. This is what is achieved when using multiple capacitors. The drawback is that resonant peaks easily occur at the resonant frequencies.

Figure 25 shows the impedance for different frequencies for the three capacitors used in the low noise amplifiers is the fiber noise cancellation system.
Notice the two resonant peaks reducing the filtering effect at these frequencies.

Component	Labeled capacitance	Approximated inductance
C1	10 µF	100 nH
C2	1 nF	5.4 nH
C3	10 pF	5.4 nH
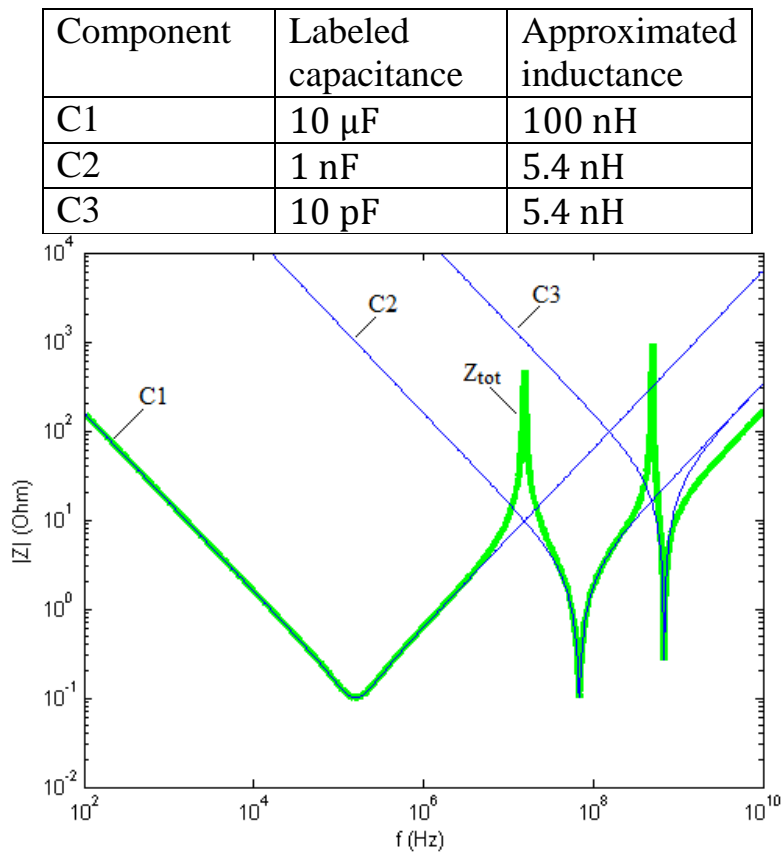
Figure 25. *Impedance simulation for decoupling capacitors, LN amplifier.*

In the two high power amplifiers for the AOMs one additional capacitor of 22 µF is connected because of the higher power consumption.

3.4 P-I regulator settings

The regulator used is a LB1005 High-Speed Servo Controller from New Focus. This is a P-I regulator designed to for example be used in laser stabilization systems.

Figure 26. *P-I regulator.*

There are many knobs on the box, and the settings are not obvious at first sight. The high impedance inputs *A* and *B* can be used as differential or single. If single input is used the unused input is auto-terminated.

The *Sweep in* BNC connection and the knobs *Center* and *Span* are used to search for locking points. This is not used in this fiber noise cancellation system where the frequency versus voltage is approximately linear.

An *Error Monitor* BNC is very useful when adjusting the settings by monitoring the signal in an oscilloscope together with the output signal. Note the current limit of 20 mA of the output that when measured by a 50 Ω oscilloscope will limit the output voltage to 1 V.

The first step of settings is to limit the output voltage avoiding damage to the VCSO. This is done by two small potentiometers, labeled *Output Voltage Limits* + and -, on the back.

The P-I corner frequency and the gain is not so straight forward to set, but basic regulation theory gives an easy way to determine the settings.
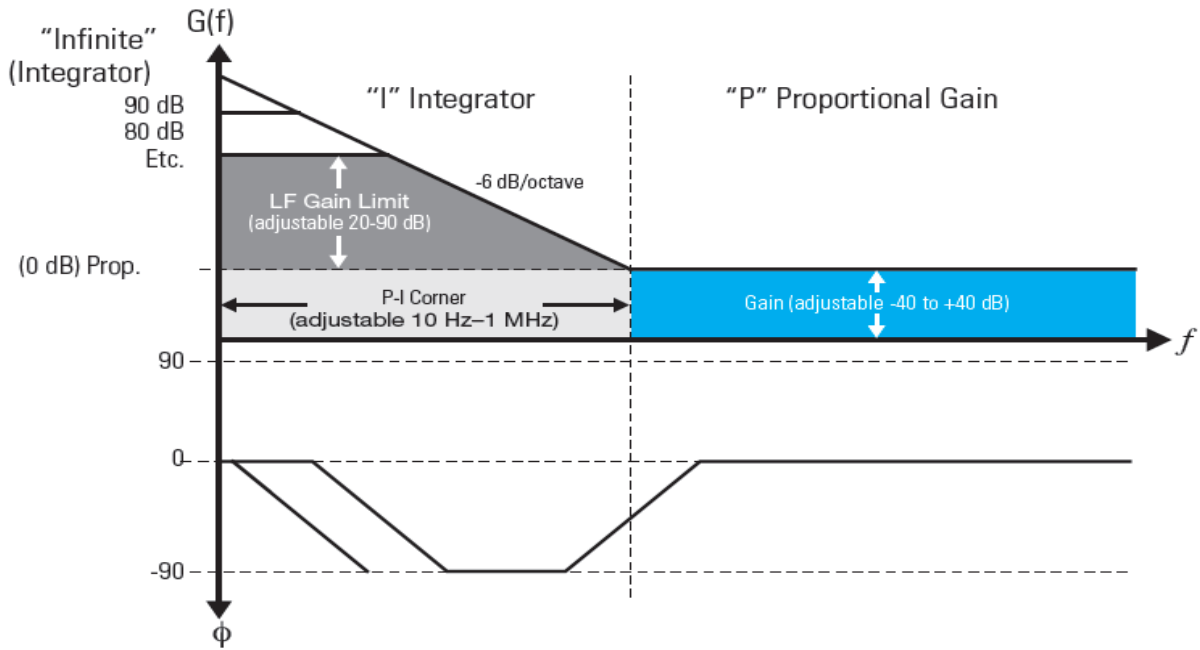
Figure 27. *Gain profile of the P-I regulator.*

To determine the gain and corner frequency values the I part of the P-I regulator should be disabled. The gain is increased to where the system is starting to self-oscillate.
The invers of oscillating frequency, T_u, and the gain, K_u is noted and by a simple formula the Integral value, T_i, and the gain, K, are calculated.

$$T_i = 0.85T_u$$

$$K = 0.45K_u$$

The mathematical function for a P-I regulator can be written

$$u_C(t) = Ku_{error}(t) + \frac{K}{T_i}\int_0^T u_{error}(t)dt$$

Where $u_C(t)$ is the controlling signal, $u_{error}(t)$ is the error signal, K the proportional constant and T_i the integral constant.

From data the P-I regulator data sheet the function of the filter gain is given in the Laplace domain.

$$V_{Control}(s) = V_{Error}(s)\frac{K'2\pi f_{PI}}{s}\left(1 + \frac{s}{2\pi f_{PI}}\right) =$$

30

$$K'V_{Error}(s) + K'2\pi f_{PI}V_{Error}(s)\frac{1}{s}$$

and when transformed to time domain

$$v_{Control}(t) = K'v_{Error}(t) + 2\pi f_{PI}K'\int_0^T v_{Error}(t)\,dt$$

From the two functions in time domain K' and f_{PI} can easily be calculated.

$$K' = K$$

$$f_{PI} = \frac{1}{2\pi T_i}$$

T_u and K_u was measured to 3.3 µs and 6.5 dB respective which gives $K' = 6.15$ dB and $f_{PI} = 57$ kHz.

4 Result

4.1 Measuring

To verify the function of the fiber noise cancellation system the original laser beam direct from the He-Ne laser is mixed by the beam passed through the cancellation system. The beam out from the fiber noise cancellation system is shifted 70 MHz by the AOM. Another AOM is connected to shift back the beam to the same frequency as the original beam, but with a 50 kHz offset. The 50 kHz beating signal is detected on a photo detector and the signal is analyzed with a oscilloscope with a FFT option.

22 different measurements was taken with varying frequency and amplitude of the simulated fiber noise generated by a signal generator connected to the piezo mirror.
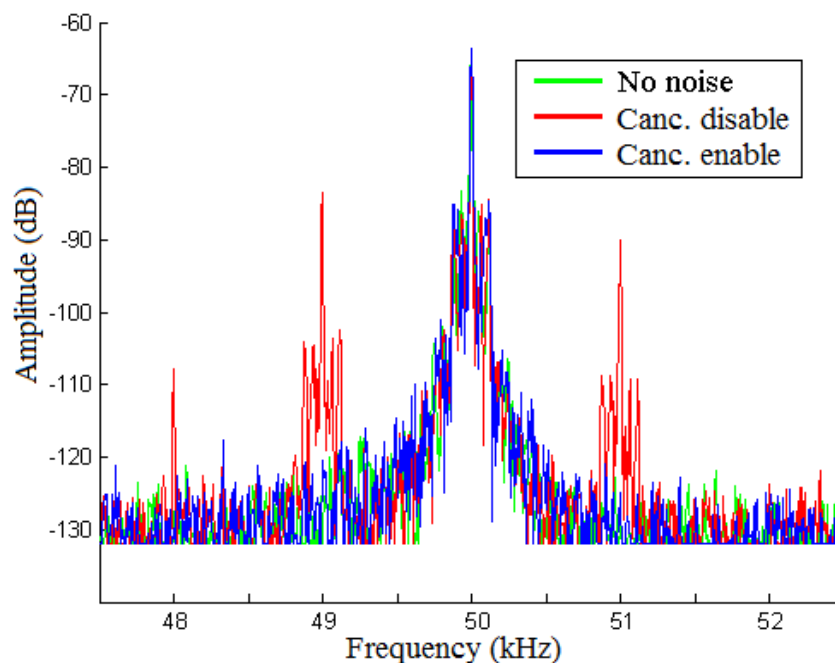
Figure 28. 50 kHz *center peak and sidebands from 1 kHz simulated fiber noise.*

Figure 28 shows measurement result when 1 kHz noise is induced to the laser beam by the piezo mirror.

The green line represents the "clean" beam where no noise is induced and the cancellation system is disabled. The red line shows when noise is applied and cancellation system not is active, and the blue line shows then the cancellation system have been activated.

The sideband peaks appears at integers of the noise frequency symmetrical to the center frequency. The stronger distortion the more and stronger sidebands appear.

32

Theoretically the peaks should be single peaks, but when zooming in at one sideband peak sub-peaks of 60 Hz are found. These peaks are present in all sidebands and the center frequency peak. The peaks are unaffected even when no noise is applied and the cancellation system is disabled.

These peaks are noticed, but no deeper investigation was taken to figure out the origin because they don't affect the measurements. In fact, this is not completely true. When simulating noise of 10 and 100 Hz, these sub-peaks makes it difficult to determine the accurate peaks and therefor the fiber cancellation at 10 and 100 Hz should be regarded with some uncertainty.
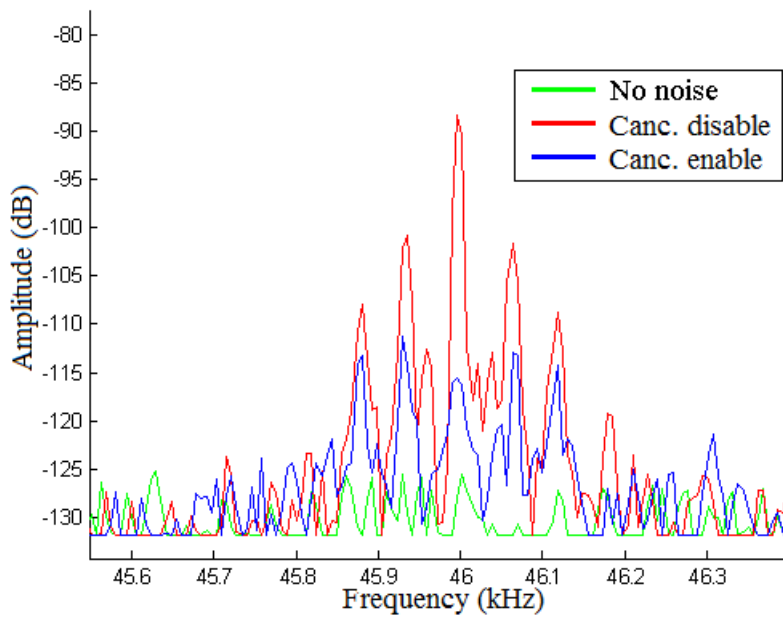
Figure 29. *Sub-peaks in one sideband peak.*

Beside of the expected sidebands there are three more alien peaks shown in *Figure 30.*
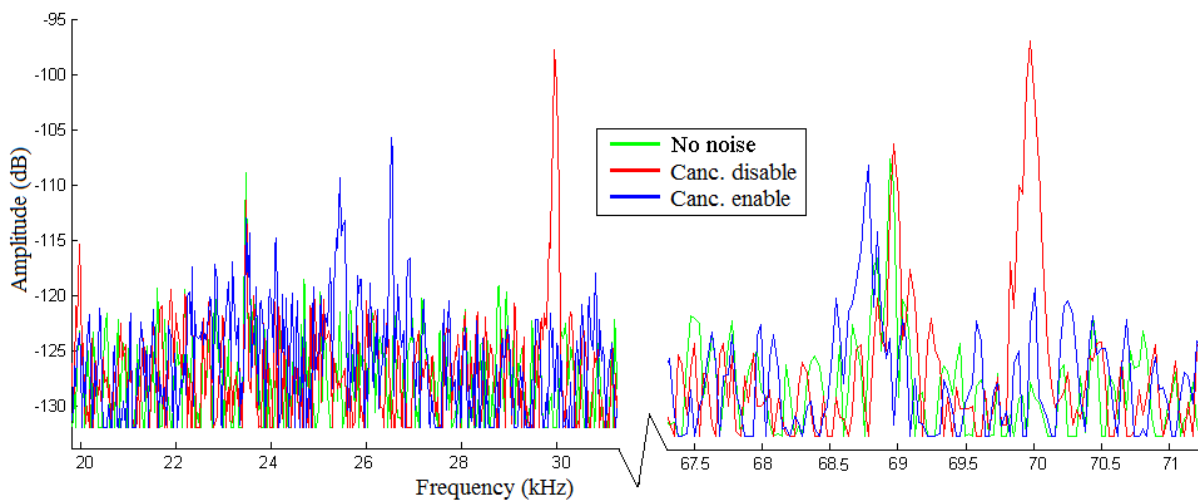
Figure 30. *Alien peaks.*

33

The peaks at 30 and 70 kHz are the second order sidebands around the 50 kHz carrier created by a 10 kHz noise, but there are one peak at 23.5 kHz and one at 69 kHz. Both these peaks are present without any applied noise and when the cancellation system is disabled.

At 25.5 kHz and 26.5 kHz the peaks is only visible when the cancellation system is enabled and must originate from it.

Some work needs to be done to investigate what causes these peaks, but this is not done in this thesis work.

4.2 Figure of fiber noise cancellation, modulation index.

It is visible just by looking at the frequency spectrum that the fiber noise cancellation system suppresses the sidebands. Another way to present the noise suppression is to use the modulation index figure.

It can be shown that the optical E-field is proportional to the voltage amplitude in the sidebands, and therefor also proportional to the Bessel functions that determine the theoretical sidebands amplitude in a frequency modulated signal.

A mathematical time dependent expression for voltage of a frequency modulated signal is

$$u(t) = A \sin\bigl(\omega_c t + m_f \sin(\omega_m t)\bigr)$$

where ω_c and ω_m is the carrier respective modulation angle frequency and m_f is the modulation index that can be seen as how much the carrier frequency is affected by the modulating frequency.

To translate this formula to sidebands amplitude is mathematically complicated, but fortunately there are certain Bessel functions that yield solutions that makes it easy to determine the magnitude of the sidebands for a given m_f.

The nth order Bessel functions can be written as a sum

$$J_n\bigl(m_f\bigr) = \sum_{m=0}^{\infty} \frac{(-1)^m \left(\frac{m_f}{2}\right)^{(2m+m_f)}}{m! \, (m + m_f)!}$$

and the five first Bessel functions is plotted below.
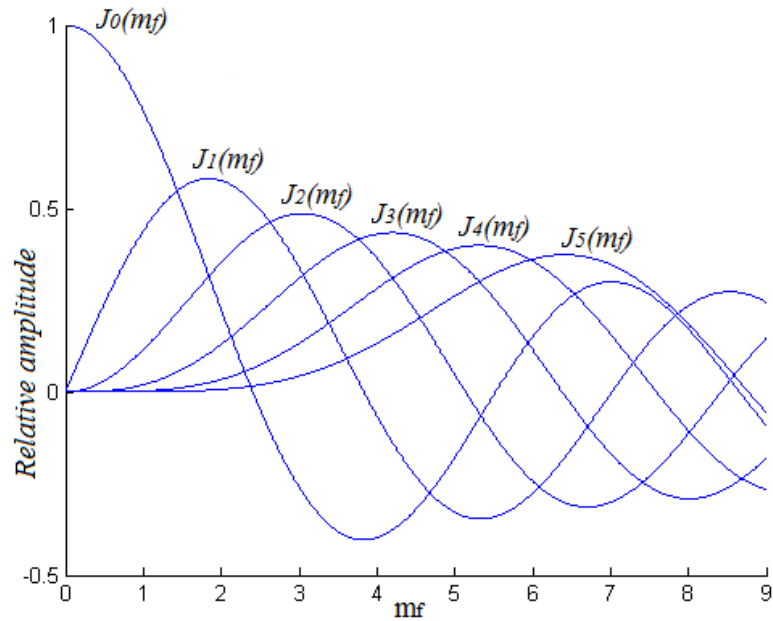
Figure 31. *Bessel functions.*

To determinate the different modulation indexes for every measurement the peaks was measured, translated from decibel to voltage and normalized. The peaks were fitted to the Bessel curves with the least square method to achieve the modulation indexes.
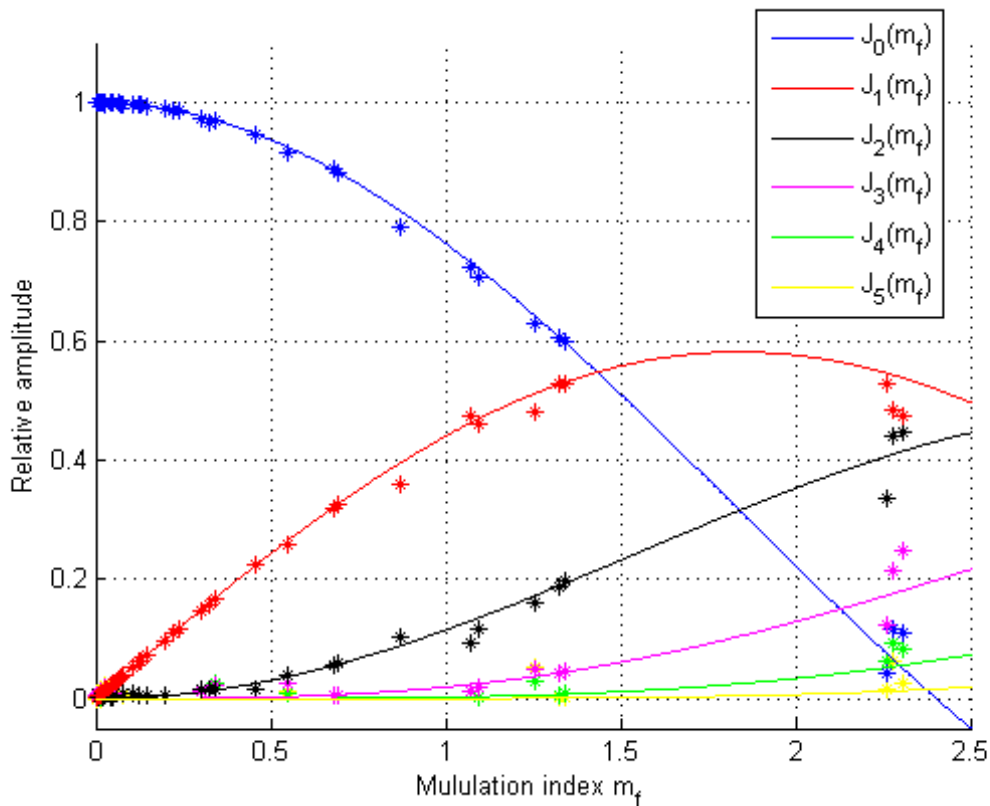
Figure 32. *Relative peak height fitted to Bessel functions.*

The measurements result for varied fiber noise simulation with varied frequency and amplitude is shown in *Figure 33 and fFigure 34*. Notice there are several different measurements at the same frequency in *Figure 33* with different simulated noise amplitude, split in graph because of clarity.
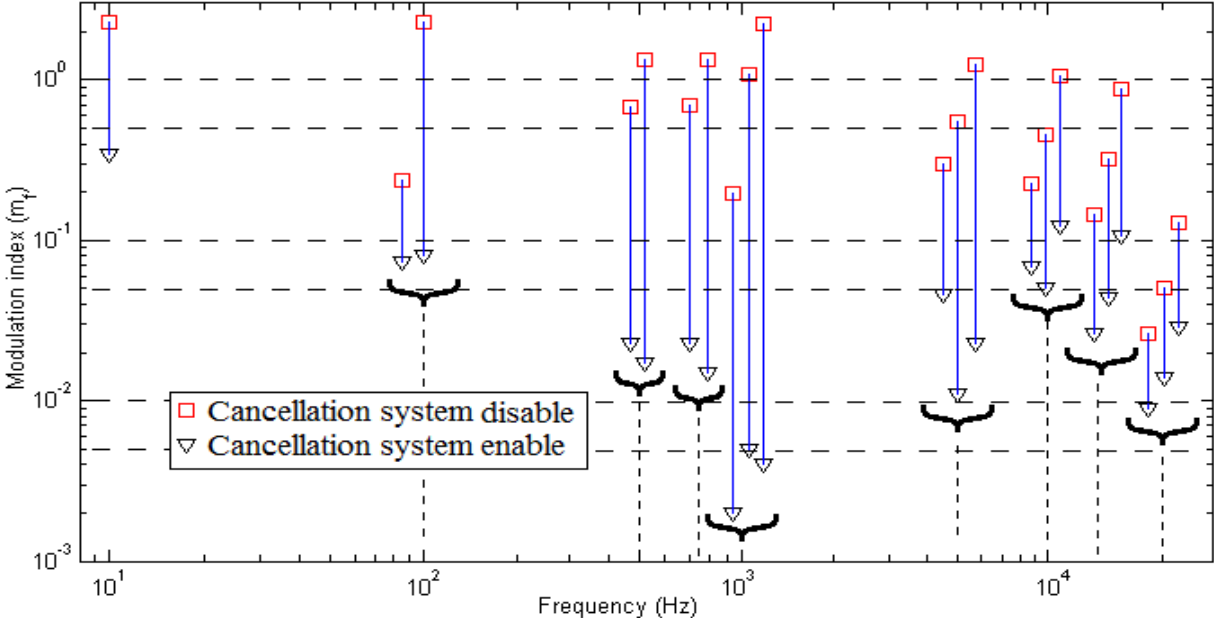
Figure 33. *Fiber noise cancellation plotted in modulation index suppression for different frequencies.*
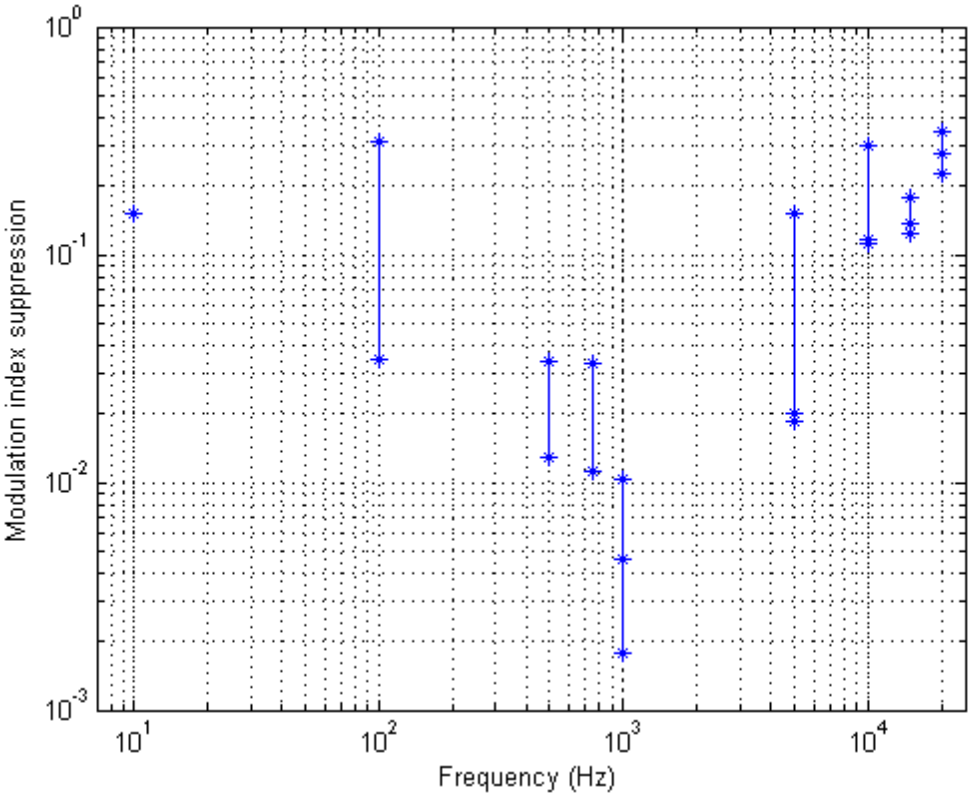
Figure 34. *Modulation index attenuation.*

36

5 Discussion

The test measurement show that this fiber noise cancellation system effectively suppress the simulated fiber noise up to 20 kHz.

To relate the suppression the result from an article with similar fiber noise cancellation system[3] is compared.

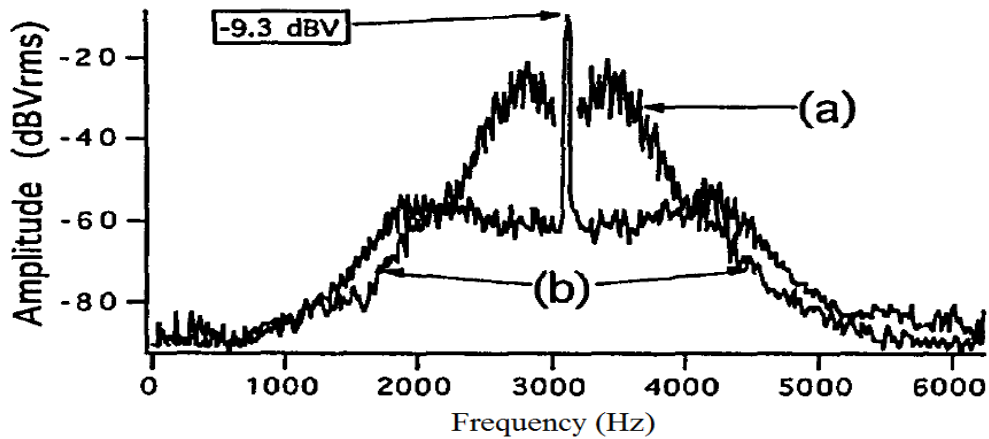**Figure 35.** *a) Cancellation disabled. b) Cancellation system enabled.*

The difference between measurement (a) and (b) is measured and plotted as the red values as a reference in *Figure 36* and is compared with the suppression at the first sideband pairs in the constructed fiber noise cancellation system, blue line.
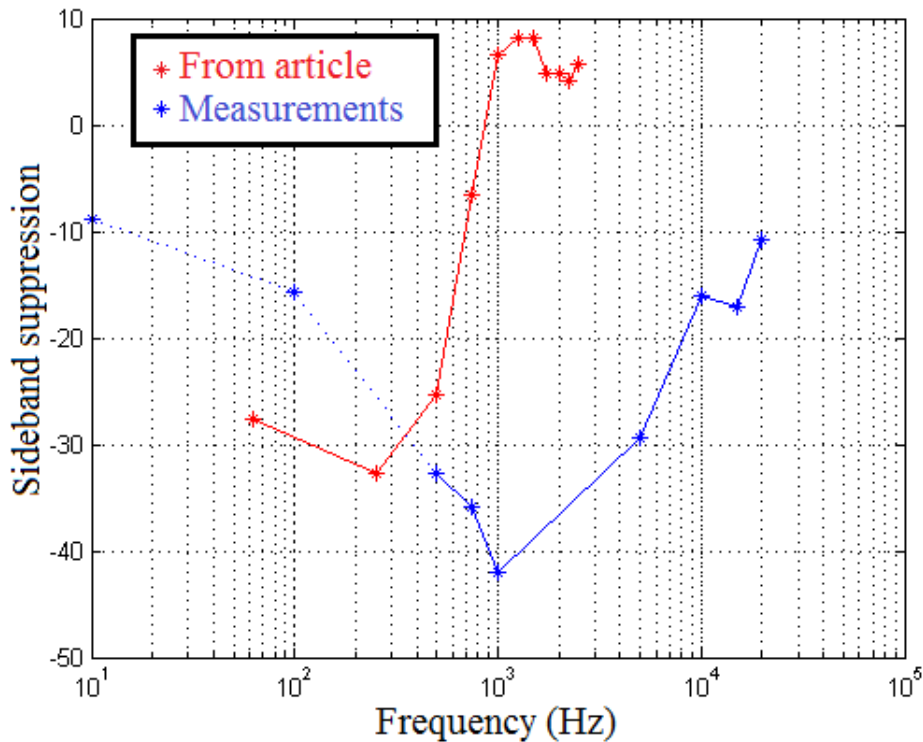

Figure 36. *First sideband suppression compared to a reference from an article.*

The suppression is about one magnitude better than the reference value for frequencies over 1 kHz. For lower frequencies the suppression from the article is better, but the attenuation for 10 and 100 Hz was very hard to measure due to noise, so this value should looked at with some uncertainty.

The bandwidth in the article system is slightly under 1 kHz for which frequency the noise instead is amplified.

The system built in this thesis work has a suppression over 10 dB for frequencies up to 20 kHz.

As so often when working with a project the time is not enough. Some things had to be skipped to get the system running within the time limits for the project. Some questions that unfortunately did not get answered were:

- What fiber noise is actually induced in an optical fiber cable?

- Where are the alien peaks come from, and how would it affect the measurements at 10 and 100 Hz if they could be cancelled out?

- It was meant to use a different faster photo detector in the system, but it was not able to work satisfactory and was replaced. Should that detector improve the performance?

- The HeNe laser used in the test system was not working properly. It was acting like jumping from high to low amplitude randomly and it was hard to adjust the P-I regulator because of the jumping. How would the cancellation system work with the 10 Hz stabilized experiment laser?

- Is the phase noise of the oscillators according to the data sheets?

6 Acknowledgments

This thesis work is the last part of my five year master of engineering nanoscience education. It's with mixed feelings I write this last sentences. Partly I'm relieved that five hard years of study has come to an end and I'm looking forward to get a job and move to a decent living bigger than my current $20\ \mathrm{m}^2$, but at the same time I'm positive that I will miss the life as a student after some time.
Yes, I have learned a lot through a numerous coursed the last five years, but I feel as the last five month working with this thesis project has been the most valuable time in my education.

I could not be happier over my choice of thesis work. I have had the opportunity to touch the exciting world of quantum computing but without to have to dig into the heavy and complex mathematics. My work has been a good mix of theory and practical work, and it's very satisfying to have been a part of a project from start to end.

I would like to finish with maybe the most important thing:
Thank you Lars Rippe as an very appreciated supervisor.
Thank you Stefan Kröll as the head of division, and of course:
Thank you all group members that never hesitated to drop your own work to assist me when I needed help.

7 Component list

Component	Manufacturer	Product nbr	Quantity	Ex quant	Unit price	Total price
Fiber noise cancelation system						
Rb frequency reference	SRS	FS725/3	1		30 822,00 kr	30 822,00 kr
DDS	Novatech	425A	1		10 088,00 kr	10 088,00 kr
DDS evaluation board	Analog devices	AD9912A/PCBZ	1		3 381,00 kr	3 381,00 kr
Box for DDS	Hammond	1550 WJBK	1		400,00 kr	400,00 kr
Mount parts for box	Elfa		1		100,00 kr	100,00 kr
Power card fo DDS	Sparkfun	PRT-10934	3		100,80 kr	302,40 kr
RS232 to USB adapter	Aten	UC-232A	2		160,00 kr	320,00 kr
Termination resistors	Vishay	D10/CRCW0402-180	2		0,24 kr	0,47 kr
Termination resistors	Vishay	D10/CRCW0402-150	1		0,24 kr	0,24 kr
Vcso	Crystek	CVS575-622.080	1		466,43 kr	466,43 kr
Capacitor for DDS	GRM	RM155R71H103KA88	1		0,11 kr	0,11 kr
Filter for DDS	Crystek	744-1359-ND	1		214,00 kr	214,00 kr
Ferrite bead	Bourns Inc.	M8696-ND	5		4,09 kr	20,44 kr
Low noise amplifier	Minicircuits	ZX60-33LN+	2		541,50 kr	1 083,00 kr
Attenuator	Minicircuits	BW-S3W5+	1		123,00 kr	123,00 kr
Power amplifier	Minicircuits	ZHL-03-5WF	1		3 353,00 kr	3 353,00 kr
Protection diode	SA	SA26A	1		3,73 kr	3,73 kr
Protection diode		5 V	2	2		- kr
Phase detector	Minicircuits	RPD2	1	1		- kr
Detector	"Jennys detector"		1	1		- kr
Filter/regulator box	New Focus	LB1005	1	1		- kr
AOM	Isomet	1205C-2	1	1		- kr
Beam sampler 10/90	Thorlabs		1	1		- kr
Beam splitter 50/50	Thorlabs		1	1		- kr
Mirrors	Thorlabs		2	2		- kr
Lens			1	1		- kr
Power supply			2	2		- kr
Computer for DDS card and Rb-ref.			1	1		- kr
For test setup						
Beam splitter	Thorlabs		1	1		- kr
Lens			1	1		- kr
Pietzo mirror			1	1		- kr
AOM	Isomet	1205C-2	1	1		- kr
Power amplifier			1	1		- kr
Attenuator	Minicircuits	BW-S3W5+	1		123,00 kr	123,00 kr
DDS	Novatech	409B	1	1		- kr
Detector			1	1		- kr
HeNe-Laser			1	1		- kr
Power supply			1	1		- kr
						- kr
Total price:						50 800,81 kr

8 References

[1] Wiman, Adam. Laser stabilization to low-expansion Fabry-Pérot cavity. Thesis work, Lund University (2011).

[2] L. K. Grover. A fast quantum mechanical algorithm for database search. Bell Labs (1996).

[3] Long-Sheng Ma, Peter Jungner, Jung Ye, John L. Hall. Optics letters Vol.19 No21. Delivering the same optical frequency at two places: accurate cancellation of phase noise introduced by an optical fiber or other time-varying path. (1994).

[4] David W. Allan. Conversion of Frequency Stability Measures from the Time-domatin to the Frequency-domain, vice-versa and Power-law Spectral Densities (2012).

[5] IDT White Paper. Voltage Controlled SAW Oscillator (VCSO) Fundamentals (2011).

[6] Nick Holland. Interfacing Between LVPECL, VML, CML, and LVDS Levels. Texas Instruments Application Report (2002)

[7] Edward B. Rosa. The self and mutual inductances of linear conductors. Bulletin of the Bureau of Standards Vol.4, No.2.